

# **IMPACT AND IMPLICATION OF THERMAL CONDITIONING ON MECHANICAL BEHAVIOUR OF FRP COMPOSITES**

*A Thesis Submitted in Partial Fulfilment of the Requirements  
for the Degree of*

**Bachelor of Technology in  
Metallurgy and Materials Engineering**



**BY:**

- 1) PRACHI SWATANTRATA JHA ,107MM001**
- 2) SWATI MITRA,107MM019**

**UNDER THE GUIDANCE OF**

**PROF. B.C.RAY**

**DEPARTMENT OF METALLURGY AND MATERIALS  
ENGINEERING  
NATIONAL INSTITUTE OF TECHNOLOGY  
ROURKELA  
769008  
ORISSA**



## National Institute of Technology Rourkela

### CERTIFICATE

This is to certify that the thesis entitled, "**Impact and Implication of Thermal Conditioning on the Mechanical behavior of FRP Composites**" submitted by **Prachi Swatantrata Jha (107MM001)** and **Swati Mitra (107MM019)** in partial fulfilment of the requirements for the award of **Bachelor of Technology Degree in Metallurgy and Materials Engineering** at National Institute of Technology, Rourkela is an authentic work carried out by her under my supervision and guidance.

To the best of my knowledge, the matter embodied in the thesis has not been submitted to any other University/Institute for the award of any Degree or Diploma.

Date:

Prof. B. C. Ray

Dept. of Metallurgy and Materials Engineering

National Institute of Technology

Rourkela-769008

## ACKNOWLEDGEMENTS

My deepest thanks to Prof. B.C. Ray sir, Department of Metallurgical & Materials Engineering, National Institute of Technology, Rourkela, the Guide of the project for constant advice and support throughout the project. Without his help, it would have been impossible to complete the thesis with perfection. I feel very lucky to have worked under him as it was a constant, once in a lifetime learning experience for me.

I express my thanks to Prof. B.B.Verma , Head of the Department, Metallurgy and Materials Engineering,N.I.T.Rourkela, for availing us the required instruments and laboratories for carrying out the project.

My deep sense of gratitude to Mrs. Shanghamitra Sethi (PhD, Department of Metallurgy and Materials Engineering, National Institute of Technology, Rourkela, for her support and guidance. She was there to help us throughout our experiments and also helped me to understand the technical aspects of my experiments.

I would also thank Mr. S.Hembram (Technical Assistant) and Mr. Rajesh Pattnaik (Technical Assistant) for giving me their valuable time when I needed it badly. Their co-operation and supervision of experiments have been vital in successful and timely completion of the project.

I would also thank my Institution and my faculty members without whom this project would have been a distant reality. I also extend my heartfelt thanks to my family and well wishers

Swati Mitra  
107MM019  
B.Tech.  
Metallurgy and Materials Engineering  
National Institute of Rourkela

Date:

Prachi Swatantrata Jha  
107MM001  
B.Tech.  
Metallurgy and Materials Engineering  
National Institute of Rourkela

Date:

## **ABSTRACT**

Fiber reinforced composites are used extensively on a very large scale. They are subject to change in temperature and loading conditions constantly. In the experimental study, we have tried to assess the impact of temperature and conditioning time on the mechanical behaviour of glass fiber reinforced composites. Interface is the most significant part of composite structure which regulates the load transfer from matrix to fiber. Its strength is measured in terms of ILSS (Inter Laminar Shear Strength). Short beam shear tests are done at ambient and 60°C for conditioning times 30 minutes, 1 hour and 3 hours. The results show that at high temperature, there is initial increase in the strength of interface up to 30 minutes followed by weakening as conditioning time increases to 1 hour. This again is followed by strengthening of the interface as conditioning time extends to 3 hours. Understanding the effect of conditioning time might help us in optimization of the mechanical properties. Composite material may contain randomly spaced microvoids, incipient damage sites and microcracks with statistically distributed sizes and directions. Therefore, the local strength in the material varies in a random fashion. The failure location as well as degree of damage induced in the material will also vary in an unpredictable mode. The fractured surfaces are photographed by SEM analysis and studied. As temperature increases, the mode of failure approaches matrix cracking, fiber breakage and debonding. Each test is carried out at six different crosshead speeds, 5mm/min, 10mm/min, 50mm/min, 100mm/min, 200mm/min, and 500mm/min. ILSS decreases as crosshead speed is increased. FTIR analysis of composite specimens was carried out to interpret the reaction between matrix and fiber at the interface. DSC analysis was done to understand the deflection of glass transition temperature with the change in temperature and conditioning time. There are a lot of conflicts over this subject and this study has tried to highlight the major factors which need to be focussed upon for further improvement in the field of composites.

# CONTENTS

Certificate	i
Acknowledgement	ii
Abstract	iii
List of figures	viii
List of tables	xii
CHAPTER 1	1
1. Introduction	2
1.2 Evolution of composites	4
1.3 Challenges	4
1.4 Objectives	5
CHAPTER 2	6
2. Literature Survey	6
2.1 FRP Composite	6
2.1.1 Fiber Reinforced Polymer Composite	9
2.1.2 Combination of fiber and matrix material	10
2.2 Fiber Reinforcements	11
2.2.1 Types of fiber reinforcements	11
2.2.1.1 Glass Fiber	11

2.2.1.1.a. Structure of glass fiber	12
2.2.1.1.b. Grade of glass fiber	13
2.2.1.1.c. Sizing of Glass Fiber	13
2.2.1.2 Carbon Fiber	15
2.2.1.2.a. Structure of carbon fiber	16
2.2.1.2.b. Characteristics and Applications of carbon fiber	16
2.2.1.3. Kevlar fiber	17
2.2.1.3.a. Structure of Kevlar fiber	17
2.2.1.3.b. Types of Kevlar Fiber	17
2.2.1.3.c. Applications of Kevlar fiber	18
2.3 Matrix Material	18
2.3.1 Function of Matrix material	19
2.3.2 Epoxy Resin	19
2.3.3 Curing of Epoxy Composite	20
2.4 Interface and Interphases	21
2.5 Effect of loading conditions on FRP composites	22
2.6 Effect of temperature on FRP Composites	23
2.6.1 Effect of temperature on glass transition temperature of	

polymers	
2.6.2 Effect of $T_g$ on mechanical properties of polymers	25
2.6.3 High temperature	25
2.6.4 Low temperature	26
2.7 Effect of moisture	26
CHAPTER 3	28
3.1 Materials	29
3.2 Experimental Procedures	29
3.2.1 Flexural test	29
3.2.2 Scanning Electron Microscopy	30
3.2.3 FTIR Spectroscopy analysis	30
3.2.4 DSC analysis	31
3.3 Experimental procedure	31
3.3.1 Fabrication of FRP Composite	31
3.3.2 Thermal Conditioning	32
3.3.3 Flexural test( Short Beam Shear Test)	32
3.3.4 SEM Examination	33
3.3.5 FTIR Analysis	34

3.3.6 DSC Analysis	34
CHAPTER 4	36
4.1 Flexural test	37
4.2 SEM analysis	53
4.3 FTIR measurements	58
4.4 DSC measurements	62
CHAPTER 5	66
5 Conclusions	67
6 Reference	68
7 Appendix	71



## LIST OF FIGURES

Fig 1	Boeing 787 dreamliner	3
Fig 2	Stress Position Profiles of fiber reinforced composites when(a) fiber length is equal to critical length(b) fiber length is greater than critical length(c ) fiber length is less than critical length	8
Fig 3	Schematic representation of FRP Composites when the fibers are (a)Continuous and aligned (b)Discontinuous and aligned (c) Discontinuos and randomly oriented	9
Fig 4	Percentage of different fiber and matrix materials used in FRP composites	10
Fig 5	Two-dimensional illustration of polyhedron network structure of sodium silicate glass	11
Fig 6	Function of the coupling agent	14
Fig 7	Variation of tensile strength and Young's modulus with heat treatment temperature for PAN based carbon fiber	15
Fig 8	Three-dimensional representation of PAN-based carbon fiber	15
Fig 9	Structure of Kevlar fiber	17
Fig 10	Photographs of different types of fibers(a)Glass fiber(b)Carbon fiber(c)Kevlar	18
Fig 11	Structure showing epoxy group	19
Fig 12	The curing of the epoxy composite	19
Fig 13	Interface between fiber and matrix	20
Fig 14	Fiber alignment due to applied stress (a) before loading (b) after loading	22
Fig 15	Stress-strain curve at different temperatures	23
Fig 16	The glass transition from glassy to rubbery state	24
Fig 17	Schematic loading configuration of three point bend test	29
Fig 18	Glass fiber reinforced polymeric composite prepared by hand lay-up method	
Fig 19	(a) Instron 1195 with short beam shear test arrangement (b)Loading of sample and	33

	fracture	34
Fig 20	.( a)FTIR spectrophotometer (b)AIM-800 Automatic Infra red Microscope	
Fig 21	(a)Mettler -Toledo 821 with intra cooler for DSC measurements (b)Reference	35
	sample chamber	39
Fig 22	ILSS Vs. Cross head speed for glass/epoxy composites at ambient temperature	
Fig 23	ILSS Vs. Cross head speed for glass/epoxy composites at 60°C temperature	40
	conditioned for 30 mins	
Fig 24	ILSS Vs. Cross head speed for glass/epoxy composites at 60°C temperature	41
	conditioned for 1 hour	
Fig 25	ILSS Vs. Cross head speed for glass/epoxy composites at 60°C temperature	41
	conditioned for 3 hours	
Fig 26	ILSS Vs. Cross head speed for glass/epoxy composites at ambient and at 60°C	42
	temperature conditioned for 30mins	
Fig 27	ILSS Vs. Cross head speed for glass/epoxy composites at ambient and at 60°C	43
	temperature conditioned for 1 hour	
Fig 28	ILSS Vs. Cross head speed for glass/epoxy composites at ambient and at 60°C	44
	temperature conditioned for 3hours	
Fig 29	ILSS Vs. Cross head speed for glass/epoxy composites at ambient and at 60°C	45
	temperature conditioned for 30mins, 1 hour and 3hours	
Fig 30	ILSS Vs. conditioning time for glass/epoxy composites at the crosshead speed of	46
	5mm/min	
Fig 31	ILSS Vs. conditioning time for glass/epoxy composites at the crosshead speed of	47
	10mm/min	
Fig 32	ILSS Vs. conditioning time for glass/epoxy composites at the crosshead speed of,	47
	50mm/min	

Fig 33	ILSS Vs. conditioning time for glass/epoxy composites at the crosshead speed of 100mm/min	48
Fig 34	ILSS Vs. conditioning time for glass/epoxy composites at the crosshead speed of 200mm/min	48
Fig 35	ILSS Vs. conditioning time for glass/epoxy composites at the crosshead speed of 500mm/min	49
Fig 36	ILSS Vs. conditioning time for glass/epoxy composites at the crosshead speed of 5mm/min, 10mm/min, 50mm/min, 100mm/min, 200mm/min and 500mm/min	49
Fig 37	Strain at Yield Vs. Crosshead Speed for samples thermally conditioned at ambient temperature	51
Fig 38	Strain at Yield Vs. Crosshead Speed for samples thermally conditioned at 60°C for 30 minutes	51
Fig 39	Strain at Yield Vs. Crosshead Speed for samples thermally conditioned at 60°C for 1 hour	52
Fig 40	Strain at Yield Vs. Crosshead Speed for samples thermally conditioned at 60°C for 3 hours	52 54
Fig 41	SEM Micrograph showing strong fiber matrix interface	
Fig 42	SEM Micrograph showing a weak interface which leads to failure mechanism of fiber pullout	54 55
Fig 43	SEM micrograph showing strong interface which leads to matrix cracking	55
Fig 44	SEM micrograph showing weak interface and the mechanism of debonding	56
Fig 45	SEM micrograph showing fiber pullout and extensive matrix damage	
Fig 46	SEM micrograph shows a strong interface giving rise to failure mechanisms like matrix cracking at 60°C for 30 minutes	56 57
Fig 47	SEM micrograph showing fiber cracking	57

Fig 48	SEM micrograoh showing fractured surface with cusps	
Fig 49	2-D micrographs taken by FTIR spectrophotometer of untreated glass/epoxy composites	59
Fig 50	2D micrographs taken by FTIR spectrophotometer of hygroscopically treated glass/epoxy composites at 1 Hr	59
Fig 51	2D micrographs taken by FTIR spectrophotometer of hygroscopically treated glass/epoxy composites at 2 Hr	60
Fig 52	2D micrographs taken by FTIR spectrophotometer of untreated, hygroscopically treated glass/epoxy composites at 1 Hr and , hygroscopically treated glass/epoxy composites at 2 Hr	60 63
Fig 53	DSC plot: Tg vs. Temperature for GFRP sample at ambient temperature	
Fig 54	DSC plot: Tg vs. Temperature for GFRP sample thermally conditioned at 60°C for 30 minutes	63
Fig 55	DSC plot: Tg vs. Temperature for GFRP sample thermally conditioned at 60°C for 1 hour	64
Fig 56	DSC plot: Tg vs. Temperature for GFRP sample thermally conditioned at 60°C for 3 hours	64
Fig 57	Bar chart showing Tg Vs thermal conditioning time at 50°C time for Glass/epoxy composites	65

## LIST OF TABLES

Table 1	Composition (wt%) of glass used for fiber manufacture	13
Table 2	characteristics and application of carbon fiber	16
Table 3	ILSS at ambient, 60°C for 30 minutes, 1 hour and 3 hours.	38
Table 4	Strain at Yield/Peak at different crosshead speeds for thermally conditioned samples for a given conditioning time and ambient samples	50
Table 5	Tg Vs thermal conditioning time for glass/epoxy composite	65

# **CHAPTER-1**

## **INTRODUCTION**

# 1. INTRODUCTION

## 1.1. Evolution of Composites

A composite comprises of two or more different materials combined together to create a superior and unique material. The first uses of composites date back to the 1500s B.C. when early Egyptians and Mesopotamian settlers used a mixture of mud and straw to create strong and durable buildings. Straw continued to provide reinforcement to ancient composite products including pottery and boats. Later, in 1200 AD, the Mongols invented the first composite bow. Using a combination of wood, bone, and “animal glue,” bows were pressed and wrapped with birch bark. These bows were was the most powerful weapon on earth until the invention of gunpowder. The modern era of composites did not begin until scientists developed plastics. Until then, natural resins derived from plants and animals were the only source of glues and binders. In the early 1900s, plastics such as vinyl, polystyrene, phenolic and polyester were developed. However, plastics alone could not provide enough strength for structural applications. Reinforcement was needed to provide the strength, and rigidity. In 1935, Owens Corning introduced the first glass fiber, fiberglass. Fiberglass, when combined with a plastic polymer creates an incredibly strong structure that is also lightweight. This is the beginning of the Fiber Reinforced Polymers (FRP) industry as we know it today. [27]

However, World War II brought the FRP industry from the laboratory into actual production. The need for lightweight and strong material applications in military aircraft led to the use of composite for military purpose. It was also discovered that the fiberglass composites were transparent to radio frequencies, and therefore it was used for sheltering electronic radar equipment (Radomes).

Later composites were used in many other applications such as production of boats and the first commercial boat hull was introduced in 1946. Brandt Goldsworthy, who is referred to as the “grandfather of composites,” developed new manufacturing processes and products.

In the 1970s the composites industry began to boost. Improved fiber as well as the matrix material was developed. DuPont developed an aramid fiber known as Kevlar, which has become the standard in armor due to its high tenacity. Carbon fiber was also developed around this time and has since been replacing metal as the new material of choice.[27]

More recently, the **Boeing 787 Dreamliner** which took its first flight on December 15, 2009 is a long-range, mid-size, body, twin jet airliner developed by Boeing Commercial Airplanes. It is the company's most fuel-efficient airliner and the world's first major airliner to use composite materials for most of its construction. [28]



*Fig 1- Boeing 787 Dreamliner[28]*



The composites industry is constantly evolving, with much of the growth is now focused around renewable energy. Wind turbine blades are constantly requiring advanced materials, designs, and manufacturing. Additionally, the composites are found to be more environmentally friendly. Resins can incorporate recycled plastics and bio-based polymers. Therefore, it is believed that composites will make the world lighter, stronger, more durable, and a better place to live.

## **1.2. Challenges-**

The material selection for a particular composite plays a very important role in the application of composite. The properties of the composite plays a very important role since the performance of the composite to be used depends greatly on its properties. However, properties come at a certain cost and this cost factor has to be balanced. Especially, the advanced materials (advanced FRP composites) always cost more as they can require extra training to learn its new design procedures and the processing can require new tooling and personnel training. Hence, the improved properties of the material must be able to justify these additional costs.

## **1.3 Objective-**

The objective of this investigation is to explore

1. The effect of thermal conditioning on glass transition temperature of the glass/epoxy composite.
2. Characterization of the interfacial interaction between the fiber and the matrix by FTIR imaging technique.
3. The implication of thermal conditioning on its propensity to change in loading speed.

4. To study the mechanical behavior of the tested samples of FRP composite by SEM micrograph.

# **CHAPTER-2**

## **LITERATURE SURVEY**

## 2. LITERATURE SURVEY

### 2.1 FRP COMPOSITE

A **COMPOSITE MATERIAL** is a **combination of two or more distinct materials, having a recognizable interface between them**. In general a composite is considered to be any multiphase material that shows a combination of properties of the two constituent phases for improved mechanical behaviour. However, most of the composites are composed of two phases; one is termed the **matrix**, which is continuous and surrounds the other phase, often called the **dispersed phase**. The fibers are classified under two broad categories. The first category of classification is based on the matrix material used. Under this category the composites are classified into 3 types i.e Metal-matrix composites (**MMCs**), Ceramic-matrix composites (**CMCs**) and Polymer-matrix composites (**PMC**). The second category of classification is based on the reinforcement used. Under this category the composites are classified into Particle-reinforced composites, Fiber-reinforced composites and Structural composites.

#### 2.1.1-Fiber-reinforced Polymer (FRP) Composite-

FRP consist of fibers embedded in a resin matrix. The properties of the fiber that affect the property of the composite are *fiber length* and *fiber orientation* in the matrix.

*Fiber-* On the basis of the length of the fiber, the fiber reinforced composites are of two types i.e. continuous and discontinuous fiber reinforced composites. Most continuous fiber (or continuous filament) composites, contain fibers that are comparable in length to the overall dimensions of the composite part. The critical length of the fiber is given as

$$l_c = \frac{\sigma_f^* d}{2\tau_c}$$

Where,  $l_c$  is the critical length of the fiber

$\sigma_f^*$  is the ultimate (tensile) strength

$d$  is the fiber diameter

and  $\tau_c$  is the fiber-matrix bond strength (or the shear strength

or the shear yield strength of the matrix, whichever is

is smaller.[2]

Fig 2 shows the effect of tensile stress on the length of the fiber. When a stress equal to the ultimate strength is applied to a fiber having just this critical length, the stress–position profile shown in Fig 2(a) results; that is, the maximum fiber load is achieved only at the axial center of the fiber. As fiber length  $l$  increases, the fiber reinforcement becomes more effective; this is demonstrated in Fig 2(b), a stress–axial position profile for  $l > l_c$  when the applied stress is equal to the fiber strength. Fig 2(c) shows the stress–position profile for  $l < l_c$ . Fibers for which  $l \gg l_c$  (normally  $l > 15 l_c$ ) are termed *continuous fiber*; *discontinuous* or *short fibers* have lengths shorter than this. For discontinuous fibers of lengths significantly less than  $l_c$ , the matrix deforms around the fiber such that there is virtually no stress transference and little reinforcement by the fiber. These are essentially the particulate composites. To affect a significant improvement in strength of the composite, the fibers must be continuous.

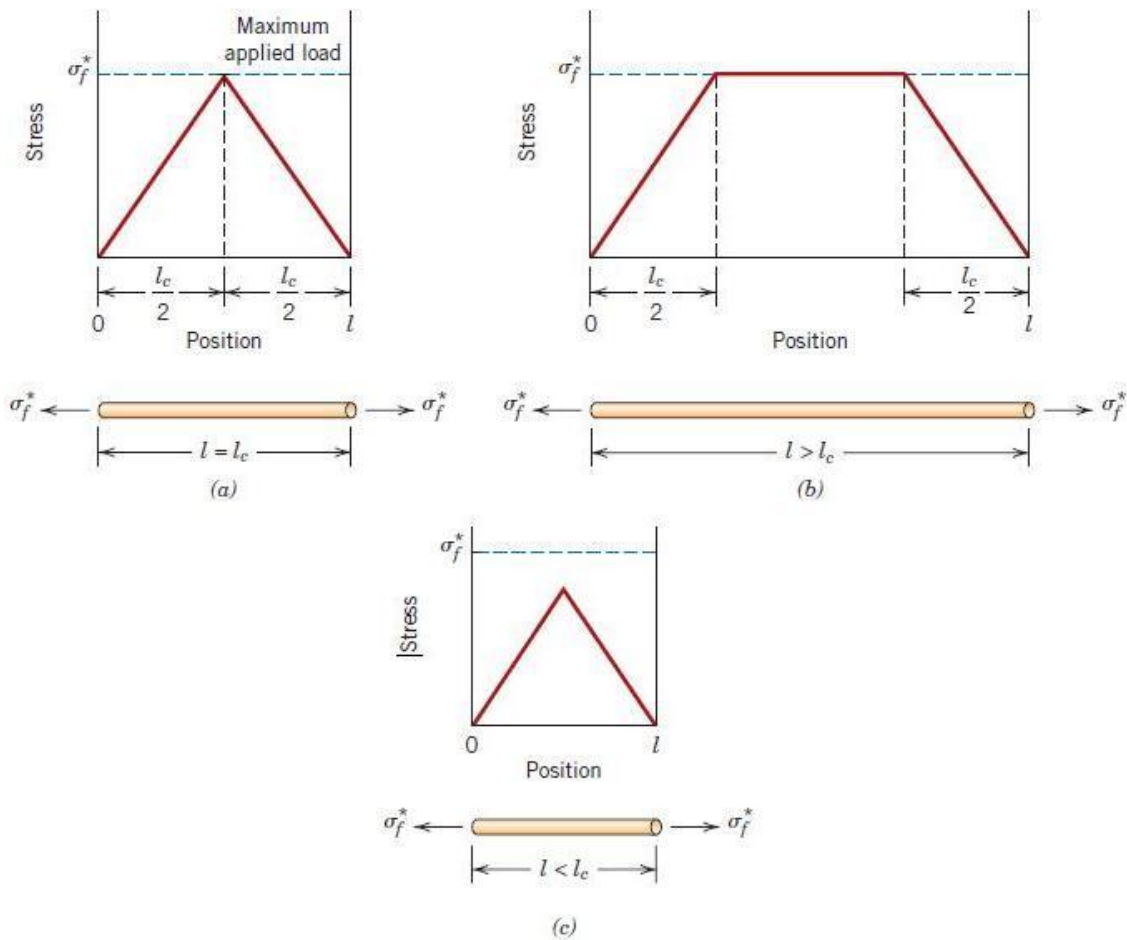
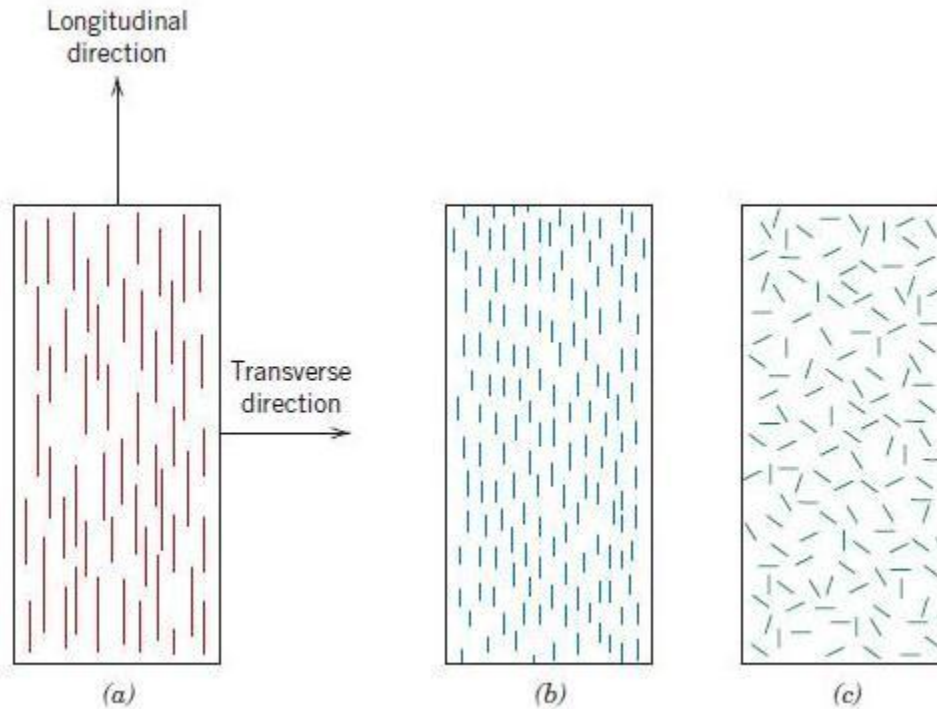


Fig 2- Stress–position profiles when fiber length  $l$  (a) is equal to the critical length  $l_c$  (b) is greater than the critical length, and (c) is less than the critical length for a fiber-reinforced composite that is subjected to a tensile stress equal to the fiber tensile strength of  $\sigma_f^*$ . [2]

The arrangement or orientation of the fibers relative to one another, the fiber concentration, and the distribution all have a significant influence on the strength and other properties of fiber-reinforced composites. With respect to orientation, two extremes are possible: (1) a parallel alignment of the longitudinal axis of the fibers in a single direction, and (2) a totally random alignment. Continuous fibers are normally aligned (Fig 3(a)), whereas discontinuous fibers may be aligned (Fig 3(b)),

randomly oriented (Fig 3(c)), or partially oriented. Better overall composite properties are realized when the fiber distribution is uniform.[2]



*Fig 3-Schematic representations of (a) continuous and aligned, (b) discontinuous and aligned, and (c) discontinuous and randomly oriented fiber-reinforced composites.[2]*

**Resin matrix-** It is an adhesive that supports the fibers from buckling under compressive stress ,binds the fibers together through cohesion and adhesion ,protects the fibers from physical and chemical attacks and micro-cracking during service, and provides shearing strengths between FRP laminas. Shearing strength is essential to resist delamination, lap joint failure and impact forces.

### **2.1.2 Combination of fiber and matrix material**

The choice of fiber and matrix material depends of specific application of the composite.

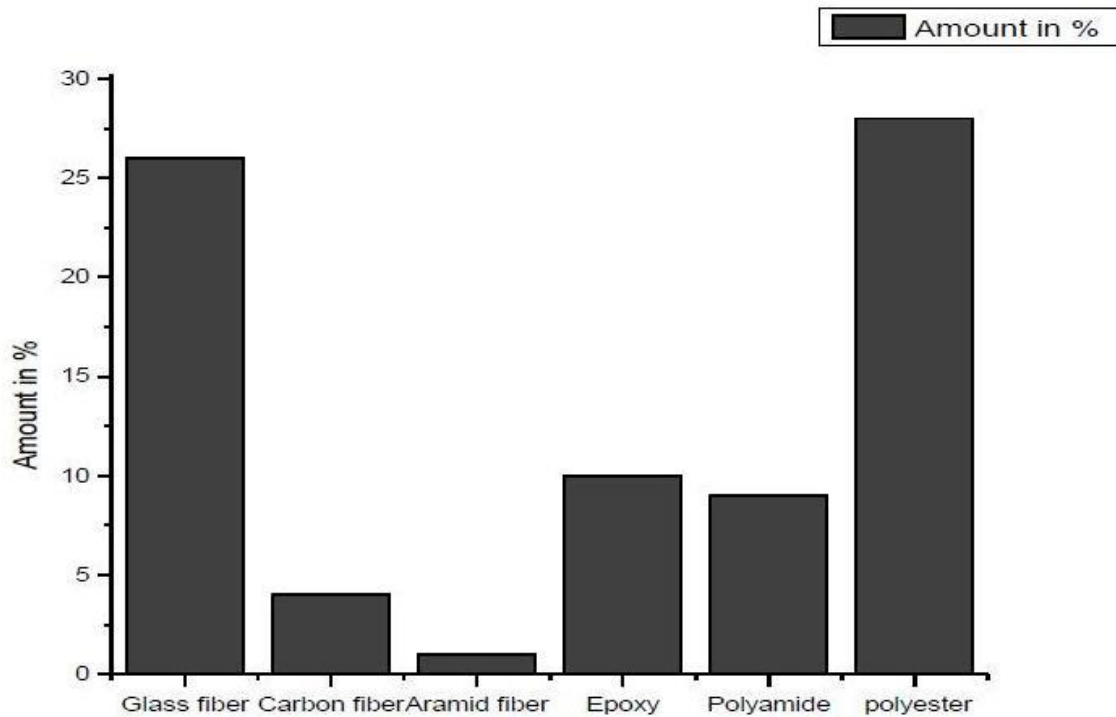


Fig 4- % of different fiber and matrix materials used in FRP composites[3]

## 2.2 FIBER REINFORCEMENTS-

Fiber-reinforced composites are technologically the most important composites. The strength of these composites is mainly determined by the fiber strength. Besides the stiffness of the composite also depends on the fiber stiffness. As optimization of the strength and stiffness has been the basic objective, the selection of fiber plays a very important role in composite manufacture.

## 2.2.1 Types of fiber reinforcements-

There are basically 3 types of fiber reinforcements used in FRP composites for commercial purposes-

- Glass fiber
- Carbon fiber
- Kevlar fiber

### 2.2.1.1 Glass fiber

It is the most common reinforcement used for Polymer Matrix Composite.

#### 2.2.1.1(a) Structure of the glass fiber

The glass fiber has a polyhedron network of sodium silicate. In this polyhedron the oxygen atoms are bonded to the silicon atoms by covalent bond whereas the Sodium ion forms a covalent bond with the oxygen atoms. This three-dimensional network in glass results in the isotropic property of glass fiber unlike Carbon and Kevlar fibers which are anisotropic.[4]

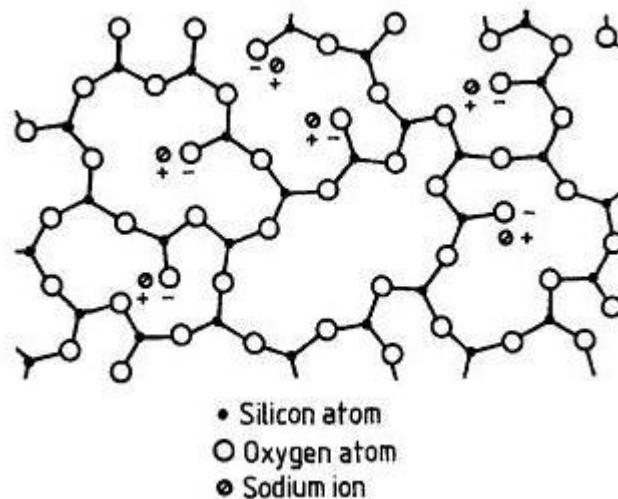


*Fig 5-Two-dimensional illustration of polyhedron network structure of sodium silicate glass[4]*



### 2.2.1.1(b) Grades of glass fiber

1. **E-Glass fiber-** The designation E stands for electrical grade. This grade of glass has low alkali content. The E-glass fibers are good electrical insulators, having good strength with moderate Young's modulus. More than 50% of the glass fiber used as reinforcement are E-glass fibers.
2. **C-Glass fiber-** C stands for corrosion /chemical grade of glass. They have better resistance to chemical corrosion than E-glass fiber. Hence, they are suitable for application in chemical plants.
3. **S-Glass fiber-** S stands for structural grade glass fiber. These glass fibers have high strength and high modulus. They are mostly used for military applications. their modulus is 20% greater and their creep resistance is also higher than E-Glass fiber.
4. **R-Glass fiber-** They are made with a calcium aluminosilicate glass. They have higher tensile strength and have higher resistance to fatigue than E-glass fiber.
5. **A-Glass fiber-** They have high alkali content which offers good resistance to chemicals but lowers its electrical property.

**Table 1- Composition (wt%) of glass used for fiber manufacture [4]**

Elements	E-Glass	C-Glass	S-Glass
SiO <sub>2</sub>	52.4	64.4	64.4
Al <sub>2</sub> O <sub>3</sub> , Fe <sub>2</sub> O <sub>3</sub>	14.4	4.1	25.0
CaO	17.2	13.4	-
MgO	4.6	3.3	10.3
Na <sub>2</sub> O <sub>3</sub> , K <sub>2</sub> O	0.8	9.6	0.3
Ba <sub>2</sub> O <sub>3</sub>	10.6	4.7	-
BaO	-	0.9	-

**2.2.1.1(c) Sizing of glass fibers**

Sizing material are coated on the surface of the glass fiber[3] immediately after forming in order to protect them from mechanical damage. For the glass fiber used as reinforcement in PMCs, sizing is usually done by a coupling agent to promote adhesion with the polymer matrix. These coupling agents are usually organosilanes of the formula X<sub>3</sub>SiR, where R is a group that can react with resin where as X is a group that can hydrolyse to form silanol group which can react with the hydroxyl group of the glass. During curing the R group reacts with the functional group of the uncured thermosetting resin, such as epoxy group in epoxy resin to form a strong covalent bond. [4,6]

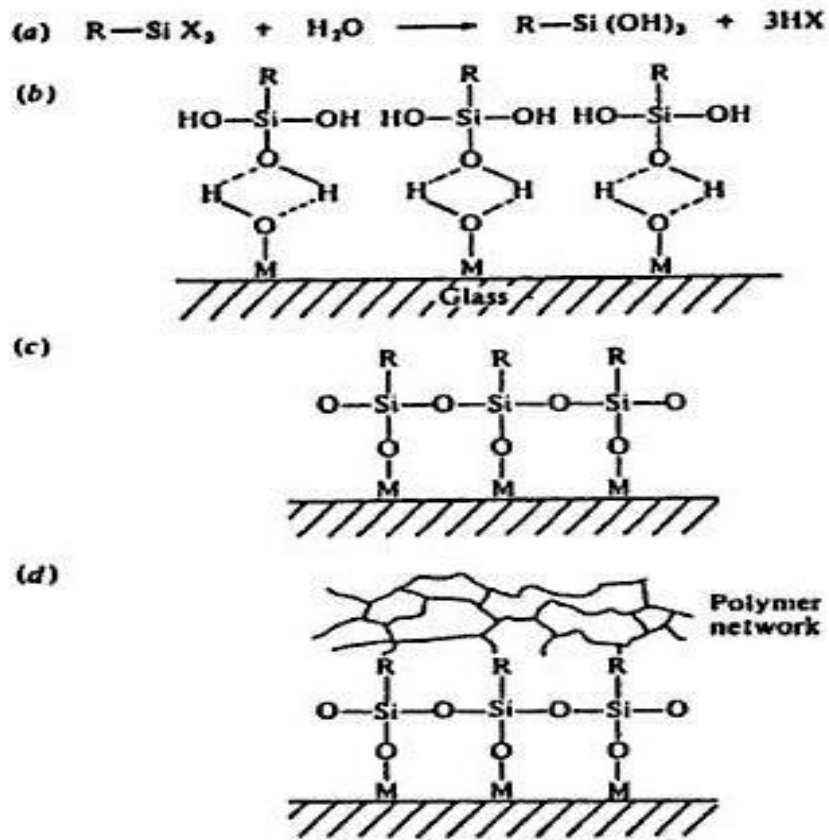


*Fig 6-Function of the coupling agent [4]*

### 2.2.1.2 Carbon fiber-

Carbon fiber have extremely high modulus value and can be made by carbonization of organic precursor fibers followed by graphitization at high temperature. The most commonly used precursor for carbon fiber is poly acrylonitrile (PAN). The carbon fiber thus produced is highly anisotropic at nanoscopic level. The density of the carbon fiber varies with the precursor and the thermal treatment given. However, it is usually in the range of 1.6-2.0. The tensile modulus and strength of the carbon fiber varies with carbonization temperature as shown in Fig 7. The increase in the tensile modulus with increase in temperature was mainly due to increase in graphitization of carbon at higher temperature. The tensile breaking strength is affected by the flaws present in the fiber.[4,7]

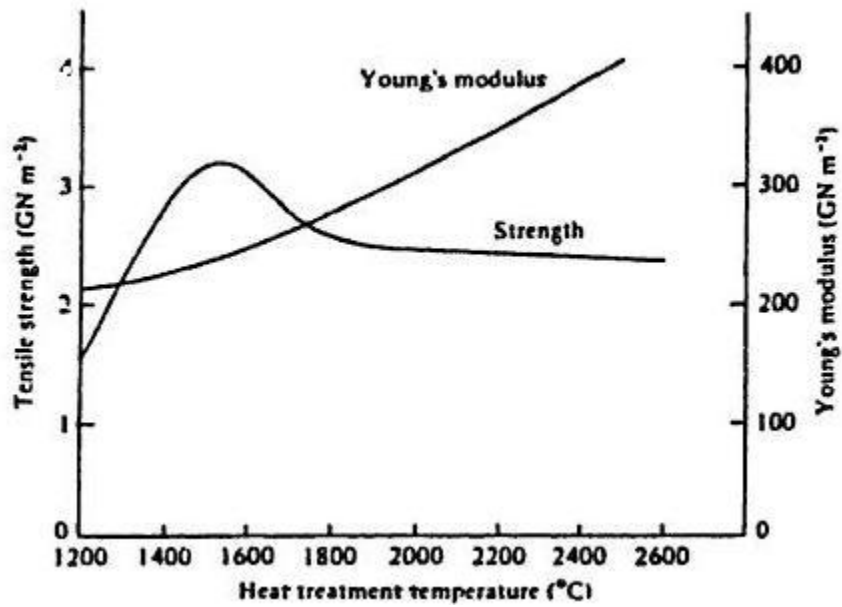


*Fig 7-Variation of tensile strength and Young's modulus with heat treatment temperature for PAN based carbon fiber.[7]*

### **2.2.1.2(a) Structure of carbon fiber**

Fig 8 illustrates the three-dimensional structure of a carbon fiber. Regions of crystallinity are separated, in a longitudinal direction, by zones of extensive bonding and twisting of basal tilt, twist and bend plane boundaries which consist of arrays of basal dislocations.

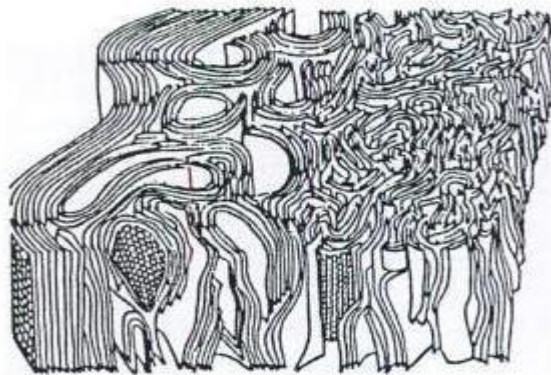


*Fig 8- Three-dimensional representation of PAN-based carbon fiber.[7]*

### 2.2.1.2(b) Characteristics and application of carbon fiber

**Table 2-characteristics and application of carbon fiber [7]**

Physical characteristics	Application
Specific strength, specific toughness, light weight	Aerospace, road and marine transport, sports goods
High dimensional stability, low co-efficient of thermal expansion, low abrasion	Missiles, aircraft breaks, aerospace antenna
Good vibration damping, strength and toughness	Audio equipment
Electrical conductivity	Automobile hoods
Biological inertness, X-ray permeability	Medical application in prostheses, surgery
Fatigue resistance, self-lubrication, high damping	Textile machinery, general engineering
Chemical inertness, high corrosion resistance	Chemical industry, nuclear field

### 2.2.1.3 Kevlar fiber

Kevlar is the commercial name of aramid fiber. Here the fiber forming substance is long-chain synthetic polyamide in which around 85% of the amide linkages are attached directly to aromatic rings. These fibers have very high modulus and are highly crystalline. They have high packing efficiency due to para orientation of the aromatic ring. The strong covalent bonding in fiber direction and weak hydrogen bonding in transverse direction result in highly anisotropic properties.[7]

### 2.2.1.3(a) Structure of Kevlar fiber

Chemically the Kevlar aramid fiber is poly (*p*-phenyleneterephthalamide) which is a poly-condensation product of terephthaloyl chloride and *p*-phenylene diamine.

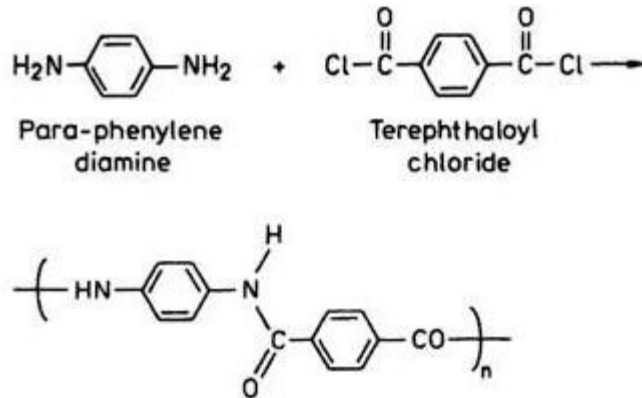


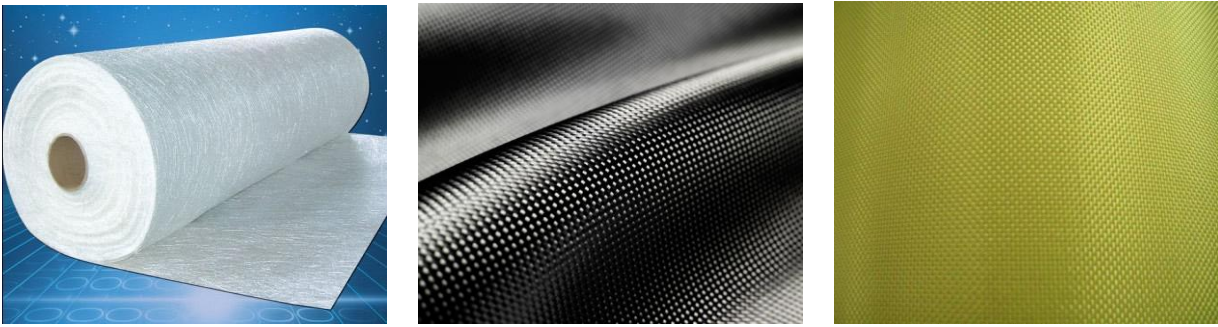
Fig 9- Structure of Kevlar fiber[7]

### 2.2.1.3(b) Types of Kevlar fiber

There are mainly three well known varieties of Kevlar fiber i.e Kevlar, Kevlar-29 and Kevlar-49.

### 2.2.1.3(c) Application of Kevlar fiber

1. *Kevlar*- It is used as rubber reinforcement for tires (belt or radial tires).
2. *Kevlar-29*- It is used for making ropes, cables, coated fabrics for inflatable and architectural fabrics.
3. *Kevlar-49*- It is used for aerospace, marine, sports and other industry. This fiber is used as a reinforcement with epoxy, polyester and other resins.[7]



(a)

(b)

(c)

*Fig 10-(a)Glass Fiber (b)Carbon Fiber (c)Kevlar Fiber*

## **2.3 MATRIX MATERIAL**

The matrix material or polymer used in FRP composites begins with a polyfunctional monomer or oligomer. On curing the liquid resin converts into a hard solid with a three-dimensional network of covalently bonded chains, which are insoluble and infusible [4]. The thermosetting resin used as matrix material are polyesters, epoxides, phenolics, polyimides etc.

### **2.3.1 Function of the matrix material**

1. It binds the fiber together.
2. Acts as medium for load transmittance between the fibers.
3. Low modulus and low strength values.
4. Protects the fibers from surface damage due to environmental or chemical factors.
5. Disperses or separates the fibers to avoid catastrophic failures by propagation of brittle cracks.
6. Establishes strong bonding with the matrix to minimize fiber pull-out and enhance stress transmittance from matrix to the fibers.[2]

### 2.3.2 Epoxy resin

Epoxy are the most extensively used matrix material for advanced Fiber-reinforced polymer composite. They are inherently brittle because of their cross-linking property. This cross linked structure provides the superior mechanical properties to the composite. The brittleness of the epoxy matrix may lead to damage in form of initiation and propagation of cracks.

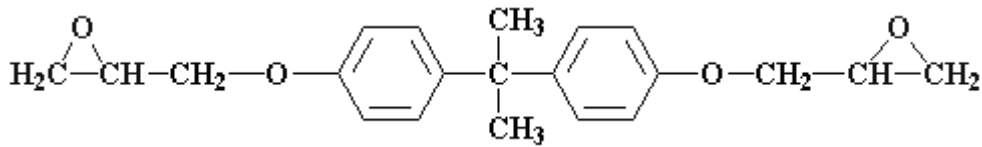


Fig 11- structure showing epoxy group[5]

### 2.3.3 Curing of epoxy composite

When the epoxy mixed with hardener is used for the manufacture of the composite, curing takes place during which cross-linking of the epoxy group takes place which in turn leads to the increase in overall mechanical behavior of the composite.[5]

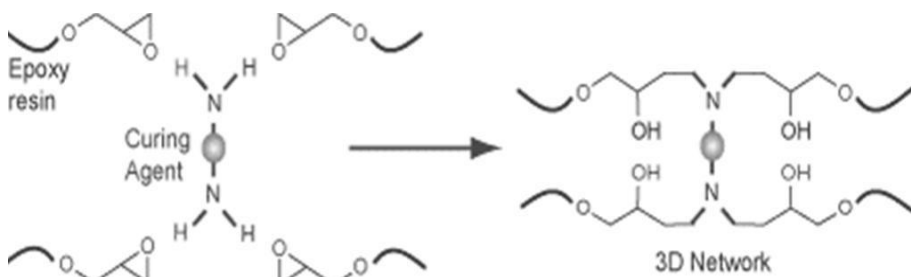
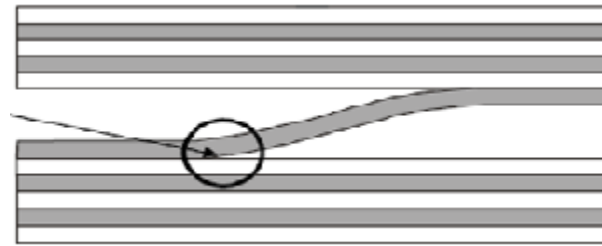


Fig 12-The curing of the epoxy composite[5]

## 2.4 INTERPHASE AND INTERFACES



The interphase is defined as a region which is manifested as a result of bonding and reactions between the fiber and the matrix.[8] Infact, this region is the site of synergy in composite materials. The successful design and the proper use of composite material depends on the intensive study of the microstructure-property relation at the interface region.[9] The structural integrity and lifetime of fibrous polymeric composites are critically depends on the stability of the fibers and the fiber/matrix interface region.[3] Besides, the mechanical properties of the composite not only depend on the fiber and the matrix materials but it strongly depends on the fiber-matrix interaction at the interface.



*Fig 13- Interface between fiber and matrix [10]*

The load transmittance from the fiber to the matrix occurs at the interface region which contributes to the strength of the composite. The interphase is a two dimensional plane having some finite thickness[4] where the chemical, physical and mechanical properties vary continuously or in a stepwise manner between the bulk fiber and the matrix materials[6]. Better the interfacial bond, better will be ILSS value, de-lamination resistance, corrosion resistance [5]. The presence of residual stresses in the interface may cause crack initiation and crack propagation in the matrix. The moisture interaction with the metal oxides in the E-glass leads to corrosion induced damage and results in reduced mechanical strength.[11]. The interaction between the fiber and the matrix material during

thermal conditioning and hygroscopic treatment are complex but they lead to the formation of interphase.[3].

## **2.5 EFFECT OF LOADING CONDITIONS ON FRP COMPOSITES**

The present report emphasizes on the various loading conditions applied to the fiber reinforced composite. The composite structure undergoes various loading conditions during their service life e.g. sports equipment which experience high loading rate to pressure vessels at low loading rates [12]. The fiber/matrix interfacial bond influences the mechanical behavior of composite because it is transmitting the load from the matrix to fibers [13]. The fiber/matrix interface mechanical properties are sensitive to the loading conditions. The de-bonding forces and apparent shear strength values increases with increasing displacement rate [14]. The failure mechanism in the GFRP laminates shifts from fiber brittle failure at low crosshead speeds, to brittle failure with extensive matrix failure as crosshead speed rises. [15]. The present investigation has been focused on the crosshead speed and temperature dependence of glass/epoxy composites. The ILSS values of the composites change noticeably when the loading rate is varied.[16] The primary failure modes in composite under high loading rate comprises of delamination via mode 1, matrix cracking via transverse shear and translaminar fracture via fiber rupture [17]. The fracture mechanisms mentioned above are dominated by the loading conditions along with material variables. When loading is done, the misaligned fiber align themselves in the direction of strain ,thereby, increasing the strength of the composite and helps the material to approach its theoretical strength within a short span of pre-stress.[18]

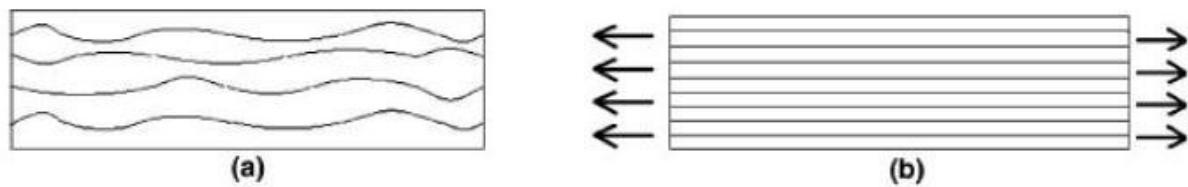


*Fig 14-Fiber alignment due to applied stress (a)before loading (b)after loading[10]*

Fig 14 shows the material with typical fiber misalignment during processing (a) and the composite material with aligned fibers after loading (b).

## **2.6 EFFECT OF TEMPERATURE ON FRP COMPOSITE**

The effect of temperature on fibrous polymeric composites is one of the most difficult challenge faced by the composite designers as it can have a vehement impact on the response of the composite material. When a material which is ductile at room temperature is subjected to rise in temperature, it attains softness and viscosity whereas at lower temperatures, it becomes brittle.[19] As a result of these fluctuations, changes in strength may be observed. The temperature dependence of matrix affects the properties of matrix. Some of these properties are compressive strength, flexural strength, shear strength.[3] When the conditioning time is small, the rise in temperature increases the interlaminar shear strength.[8] Thermal degradation of resin matrix involves chemical reaction and physical changes. The chemical reactions occurring are oxidation, further cross-linking and reaction between monomers, while physical phenomenon are viscoelastic deformation.[20] The visco-elastic yield behavior is affected by the temperature and loading rate. Chain scission and cross-linking reactions affect the polymer network thereby altering the mechanical behaviour of the oxidized layer. At the macroscopic level, oxidized layer shrinks ,inducing a stress gradient that might initiate and propagate cracks [21]. Thermal conditioning behavior of glass fiber epoxy composite is of special interest, because of their extensive structural applications at high temperature environmental conditions. The

fracture mechanism of polymer resin depends on the yielding phenomenon which is temperature and time dependent. At very low temperature the fracture is brittle as no yielding is possible. However, at high temperature two characteristic mechanisms are possible after the attainment of yield point, namely, strain softening and strain hardening. A greater level of micro-cracking and de-lamination is visible at low temperatures, which may be due to higher thermal residual stresses [20]. thermal stresses are generated due to differential co-efficients of thermal expansion and contraction of matrix and fiber. The fiber/matrix interface becomes weak due to which their ILSS values decrease progressively.[3]

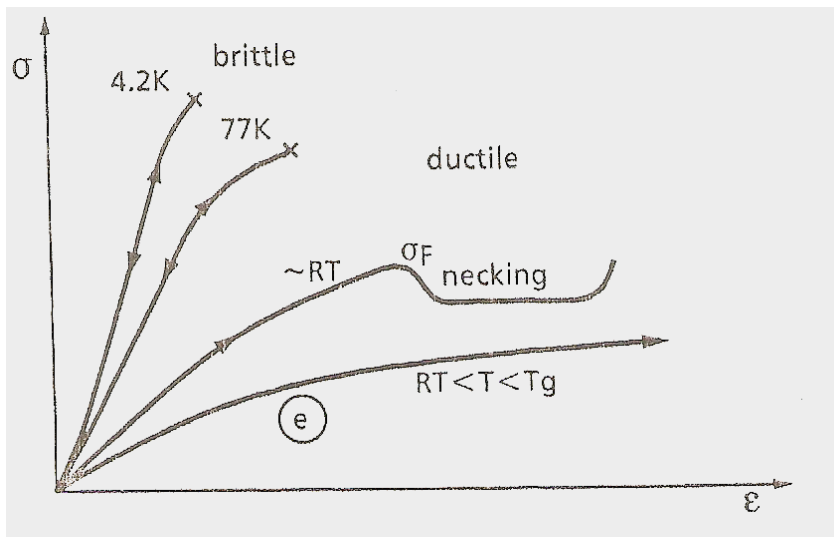
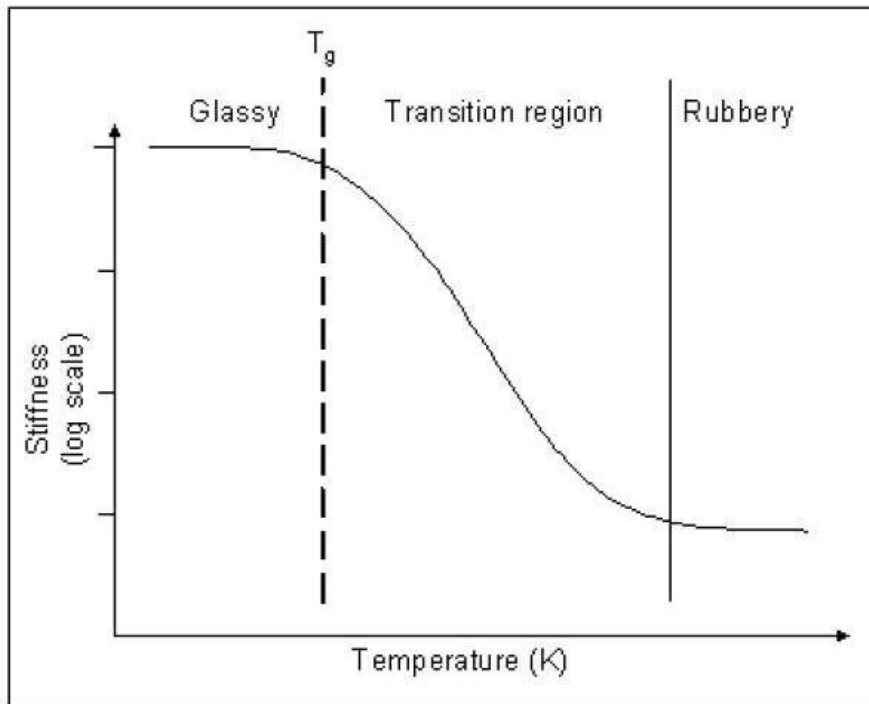


Fig 15-Stress-strain curve at different temperatures[22]

### 2.6.1 Effect of temperature on Glass transition temperature of polymers

The temperature at which the polymer undergoes transition from rubbery to glassy or rigid states is known as the **glass transition temperature,  $T_g$** . The glass transition takes place over a range of temperature as shown in Fig 16. Generally, the range varies from 0.5 to 0.8  $T_m$ (in Kelvin) [2]



*Fig 16-The glass transition from glassy to rubbery state[28]*

Below  $T_g$ , the polymer acts as stiff and glassy solids and low energy brittle failure becomes the main cause of failure. High temperature above  $T_g$  act as softening agent and decreases the strength and stiffness as the polymer chain mobility increases. However, the glass transition results in only a partial softening because of high level of crosslinking in the polymer matrix. The factors that effect the range of the region in which the glass transition occurs are as follows

1. Resin composition
2. Temperature
3. Curing time
4. Cross-linking density of polymer
5. Polar nature of the polymer
6. Molecular weight of the polymer

### **2.6.2 Effect of Tg on mechanical properties of polymer**

The mechanical behavior of composites depends on the ability of interface to transfer stress from the matrix to the reinforcement fiber.[8] Tg can be used to evaluate the response of polymeric material to mechanical stress. Polymers above their Tg will exhibit visco-elastic behavior and are found to be dimensionally stable while the polymers which are below their Tg exhibit brittle behavior and are less dimensionally stable. As the cross-link density is increased due to higher polymerization, molecular motion becomes more restricted and the Tg of the cross-linked polymer chain rises. Hence, the modulus also increases.[23]. It is generally believed that higher the Tg, better the mechanical properties.

### **2.6.3 High temperature**

Thermal conditioning at a temperature above Tg improves adhesion level at the interfaces. Adhesion chemistry is influenced by post-curing phenomena which increase with more conditioning time. Fiber breakage, fiber/matrix interfacial fracture and de-lamination between adjacent plies of the laminates are some of the failures which are observed in the FRP composites. Due to these fractures, the inter-lamellar shear strength may decrease with increasing temperature. Thermal conditioning is likely to affect the chemistry at the fiber/matrix interface and imparts higher polymerization with the development of penetrating and semi-penetrating network at the fiber-matrix interface.[3] This imparts better adhesion and thus an improved ILSS values especially at the less conditioning time. However, at high temperatures above the glass transition temperature (Tg), fiber reinforced polymeric composites are susceptible to thermo-oxidative degradation. Fibers are unaffected by the temperatures below Tg but the polymer matrix and the interface are degraded resulting in deterioration of physical and mechanical behavior of the composite. [24]. The response of fiber/matrix interface is significant in determination of the gross mechanical behaviour as the load is transmitted from the matrix to the fiber

at the interface which contributes to the composite strength. The interfacial bond better is directly related to the ILSS, and resistance to delamination, fatigue and corrosion resistance.[3]

#### **2.6.4 Low temperature**

Now-a-days intensive research of polymeric material for cryogenic applications are been carried out because of their specific use in cryogenic environments. Localized surface degradation, de-lamination, and micro-cracking are few of the most frequently observed damage mechanisms which may develop in polymer composites on exposure to cryogenic temperatures. Cracks and delaminated areas are produced as a result of misfit strains at the interfaces due to differential coefficient of expansion between fiber and polymer matrix. Besides, crazing may also occur in lightly cross-linked thermoset resin but not in well cured epoxy resins.[8] . The reduction in shear strength during cryogenic treatment may be because of the the weakening of interfacial bond. However, hardening at cryogenic temperatures may modify the local threshold which is required for the breakage of adhesive bonds at the interface. [8]. Besides, low temperature strengthening may also occur due to mechanical keying at the fiber-matrix interface.[29] During cryogenic treatment, compressive residual stresses may develop due to differential thermal contraction which influences the overall thermo-mechanical behaviour of the composite. Sometimes, these stresses initiate plastic deformation in the matrix around the fiber. The thermal residual stresses may also initiate material damage like matrix micro cracking. These micro cracks decrease the stiffness and the strength in the material, and also act as sites for microcrack nucleation [25]. Hence, after low temperature treatment, the cross-linked polymers show brittle behavior as it doesn't allow relaxation of the thermally induced residual stresses.

#### **2.7 EFFECT OF MOISTURE**

The amount of environmental degradation occurring in a fiber reinforced polymer composite structure is varies directly with the amount of moisture absorbed.[3]. Water absorption in polymer matrix at room temperature and above acts as a softening agent but at cryogenic temperatures, the matrix resin

becomes stiffer than the dry ones.[26] The amount of water absorbed at the interface depends upon the nature of the glass surface, lower the functionality of the silane, higher the cross-link density at the interface and lesser will be the amount of moisture absorbed.[29]. Moisture may penetrate into the polymeric composite by diffusion or by capillary process. The Fick's law of diffusion predicts the rate of water absorption, where the moisture content at a particular instant of time is proportional to square root of time wherein,  $Dt/h^2 < 0.05$ .[3]. The amount of moisture absorbed by the matrix resin is significantly different than that of the reinforced fiber. This in turn results in a significant mismatch in the moisture induced volumetric expansion between the matrix and the fiber and leads to the evolution of localized stress and strain fields in the composite.[30]. The moisture penetration also results in plasticization of the resin matrix which induces plastic deformation in addition to lowering of glass transition temperature. Besides the moisture interaction with the metal oxide in the E-glass leads to corrosion induced damage and thus results in reduced mechanical strength.[31,32].



# **CHAPTER-3**

**MATERIALS**

**EXPERIMENTAL METHODS**

**EXPERIMENTAL PROCEDURES**

### 3.1 MATERIALS

Matrix is made up of epoxy and hardener. Epoxy used here is resin LY-556 which is an unmodified liquid epoxy resin and is based on Bisphenol A. Hardener used is HY 951 (aliphatic primary amine). The function of hardener is to provide low viscosity and solvent free room temperature curing laminating system. Fiber reinforcements used comprise of Woven roving E glass fibers treated with silane. The fibers are PAN based high strength. The ratio of fiber and matrix is 60:40.

### 3.2 EXPERIMENTAL METHODS

#### 3.2.1 Flexural test

The polymeric composites are subjected to three point bend tests. The tests are carried out in Instron 1195 tensile testing machine as shown in Fig 19. It is a three point flexural test. The crosshead speed is varied for each set of sample conditioned for a given time. Short span length is taken with a loading fixture as shown in fig 17. The bending load on the beam generates shear stress. The shear stress causes interlaminar shear failure. The shear stress is independent of span length and varies directly with the magnitude of applied load. Two types of failure might occur: bending and interlaminar shear. In order to attain interlaminar failure before bending, we keep a short span length.

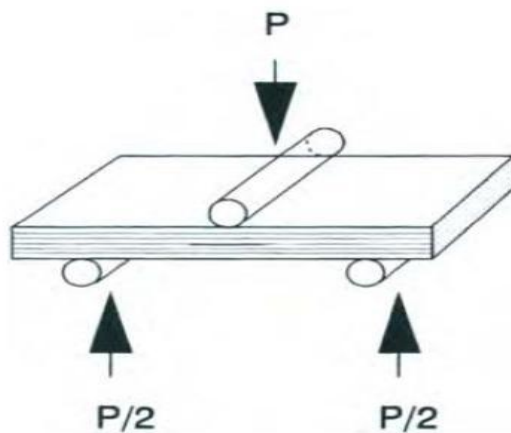


*Fig 17-Schematic loading configuration of three point bend test*

#### 3.2.2 Scanning Electron Microscope (SEM)

The scanning electron microscope (SEM) has been extensively used for examination of fracture surfaces.

It provides large depth of focus and enables us to examine the actual surfaces.

**Principle:** An electron beam which is finely focussed on the surface of the sample generates secondary electrons, backscattered electrons, as well as characteristic X-rays. The detectors collect these signals and images are formed on the screen of cathode ray tube. Through the SEM images, the elemental compositions are analyzed using EDS or WDS. The electrons emitting from the specimen surface have a spectrum of energy levels and according to these energy levels, secondary and backscattered electrons are separated. The energy level of the secondary electron is less than about 50eV whereas the backscattered electrons exit the specimen with energy greater than 50eV. The fractography of the FRP composites using SEM helps in understanding different failure mechanisms. When the composite is exposed to low and high temperatures, there is a dramatic change in the structure and properties of the composite.

### **3.2.3 FTIR Spectroscopy analysis**

**Principle:** In Fourier Transformed Infrared Spectroscopy, infrared radiations are passed through a sample. During this process, some of the radiations are absorbed while some are transmitted by the tested sample. The molecular absorption and transmission of the sample is represented by the resulting spectrum. No two molecular structures produce the same spectrum as in case of fingerprint. Hence, the infrared spectroscopy becomes useful for analysis of various kinds. Through this spectroscopy technique, various structural information for organic compounds can be obtained. The region is divided into the functional group region 4000-1300  $\text{cm}^{-1}$  as well as the finger print region 1300-650  $\text{cm}^{-1}$ . In the spectrum, most of the absorption bands of the functional groups are obtained in the high frequency range. The FTIR image analysis reveals a variation in the chemical structure of constituent matrix and the fiber of the composite.

### **3.2.4 Differential Scanning Calorimetry (DSC)**

**Principle:** Differential scanning calorimetry (DSC) is a thermo analytical technique in which the amount of heat required to increase the temperature of a sample and reference is measured as a function of temperature. Here, same temperature of both the sample and the reference is maintained throughout the experiment.

## **3.3 EXPERIMENTAL PROCEDURE**

### **3.3.1 Fabrication of FRP composite**

The glass fiber sheets are cut into predetermined dimensions of 16cm \* 16 cm. 16 such square mats were cut out from the roll of glass fiber mat. The weight of the glass fiber mats was measured. Weight of the epoxy resin taken is 60% of the weight of glass fiber. And the hardener taken has to be 10% of the weight of the epoxy. The two were mixed gently to avoid formation of air bubbles. Two mold sheets were taken and the mold releasing spray was applied on one of them (base) to prevent any tackiness during separation and for superficial smoothness. The binder mixture was spread evenly on the mold using a brush in a uniform direction and orientation. On the binder spread, glass fiber mat was put and they were rolled down onto the mold to generate an intimate contact between the fiber and the binder without any air bubbles and voids. The direction of rolling has to be in same orientation too. The resin and hardener mixture was reapplied on the first fiber mat and the same process was repeated till 16 mats were put. After the last mat is put, the mixture is spread onto it and the mold sheets were put on it after application of mold release spray. The mold was left for curing for 3 days. After the third day, the mold sheets were separated from the composites and the surface of composite was observed for defects.



*Fig 18-Glass fiber reinforced polymeric composite prepared by hand lay-up method*

### **3.3.2 Thermal conditioning**

Some of samples were put in an oven at +60°C for three different times i.e 30mins, 1hr and 3hrs for thermal conditioning.

### **3.3.3 Flexural test (Short beam shear test)**

The flexural tests are performed on the composite samples at room temperature as well as the conditioned temperature to evaluate the value of the inter-laminar shear strength (ILSS). It is basically a 3-point bend test, which promotes failure by inter-laminar shear. This test is conducted in Instron 1195 tensile testing machine as per the ASTM standard D2344-84 which is shown in Fig 19(a). The loading arrangement is shown in Fig 19(b) .The tests were performed with five increasing crosshead speed ranging from 5, 10, 50, 100, 200 and 500 mm/min. For each crosshead speed, 3 specimens were tested and the average value was taken.



*Fig 19 (a)-Instron 1195 with short beam shear test arrangement (b) Loading of sample and fracture during SBS Test*

The ILSS value is calculated according to the following equation

$$\text{ILSS} = (0.75 * P) / (b * d),$$

Where, P= maximum load at displacement

b= width of the specimen

d= depth of specimen

### **3.3.4 SEM Examination**

The fractured surfaces have to be observed in order to understand the mode of failure and effect of conditioning on the composites. For this the tested fractured samples were first prepared for SEM analysis. Then they were put in the oven at 80 degrees for 1 hour in order to remove the impurities in the surface so as to obtain a noise free image. The fractured surfaces were then observed and their images were taken. The SEM machine used was JEOL-JSM 6480 LV SEM. Vacuum was created inside the chamber after putting the samples on the sample holder. The working distance was adjusted and photographs of the area under concern were captured.

### 3.3.5 FTIR Analysis

First of all hygrothermal treatment of the composite sample to be analyzed is given for 1 hour and 2 hours at 60°C. FTIR analysis was performed in FTIR spectrophotometer interfaced with IR microscope operated in reflectance mode. The microscope has a video camera, a liquid nitrogen-cooled mercury cadmium telluride (MCT) detector and a computer controlled translation stage, programmable in the x and y directions. The spectra were collected in the 4000cm<sup>-1</sup> to 650cm<sup>-1</sup> region with 8 cm<sup>-1</sup> resolution, 60 scans and beam spot size of 20µm- 100µm. The spectral point by-point mapping of the interface of the composites was performed in a grid pattern with the use of computer controlled microscope stage.



(a)



(b)

Fig 20-(a) FTIR spectrophotometer (b) AIM-800 Automatic Infra red Microscope

### 3.3.6 DSC Analysis

The DSC analysis was performed in Mettler-Toledo 821 with intra cooler, using the STAR software. The temperature calibration and the determination of the time constant of the instrument were performed by standards of In and Zn, and the heat flow calibration by In.: The underlying heating rate used was 10°Cmin<sup>-1</sup>. In order to calibrate the heat flow signal, a blank run with an empty pan on the reference side and an empty pan plus a lid at the sample side was performed before the sample

measurements. Standard aluminum pans were used. The experiments were performed in the temperature range from 25°C to 120°C.



(a)



(b)

*Fig 21-(a)Mettler -Toledo 821 with intra cooler for DSC measurements (b)Reference sample chamber*



# **CHAPTER-4**

## **RESULT AND DISCUSSION**

#### 4.1 Flexural Test (Short Beam Shear Test)

The three point bend test/Short Beam Shear Test/ Flexural Test was carried out for the composite samples at 60°C for different holding times and at ambient temperature at varying crosshead speeds.

The ILSS values were calculated from the formula:

$$\text{ILSS} = (0.75 * P) / (b * d),$$

Where, P= maximum load

b= width of the specimen

d= depth of the specimen

Three parameters are of chief importance:

1. Crosshead speed
2. Temperature
3. Conditioning time

We plot ILSS versus crosshead speed for ambient and 60°C at different condition times. The mode of failure in flexural test is interlaminar shear. So the ILSS values indicate the degree of adhesion between the fibre and matrix.

**Table 3-ILSS at ambient, 60°C for 30 minutes, 1 hour and 3 hours.**

<b>Crosshead speed(mm/min)</b>	<b>ILSS,ambient (MPa) Avg. value on 3 test data</b>	<b>ILSS,60°C, 30 min(MPa)</b>	<b>ILSS,60°C,1 hr (MPa)</b>	<b>ILSS,60°C,3hrs (MPa)</b>
<b>5</b>	26.8155	45.345	20.682	37.94
<b>10</b>	53.639	53.045	22.8	60.089
<b>50</b>	43.719	50.21	16.392	57.206
<b>100</b>	47.79	46.246	20.586	53.82
<b>200</b>	47.797	55.342	15.327	49.23
<b>500</b>	22.946	21.175	23.028	60.4717

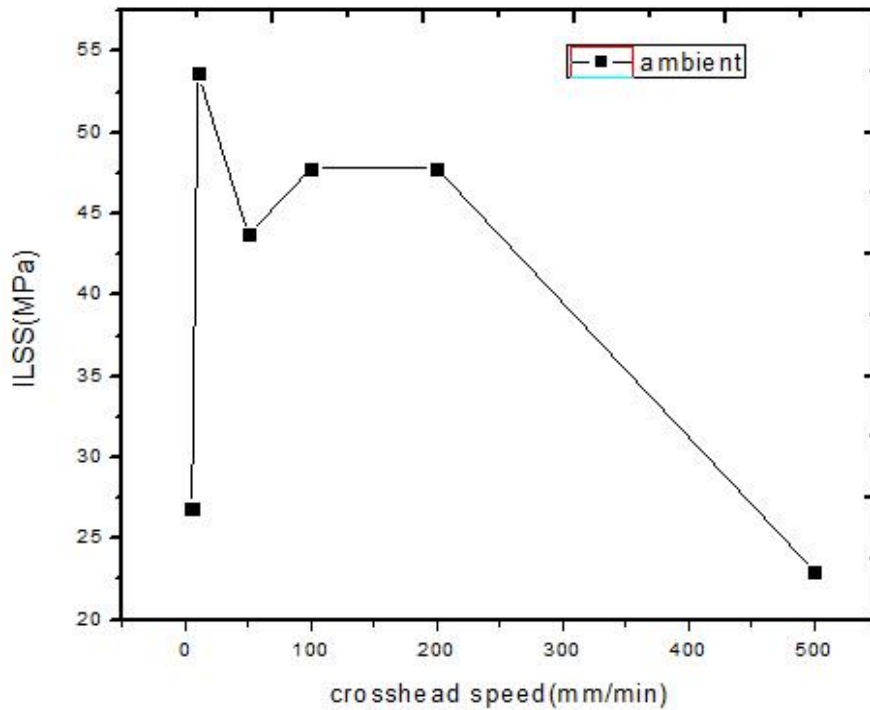


*Fig 22- ILSS Vs. Cross head speed for glass/epoxy composites at ambient temperature.*

ILSS values with varying crosshead speeds for specimens at ambient temperature is shown in Fig 22. It is taken as standard. At ambient temperature, at quasistatic crosshead speed, i.e. 5mm/min, 10mm/min, initially the ILSS value increases but as crosshead speed approaches 100mm/min, there is a decrease in ILSS (fig 22). The same pattern is followed by ILSS of the specimens conditioned at 60°C for 30 minutes, 1 hour and 3 hours as shown in fig 23, 24, 25, respectively.

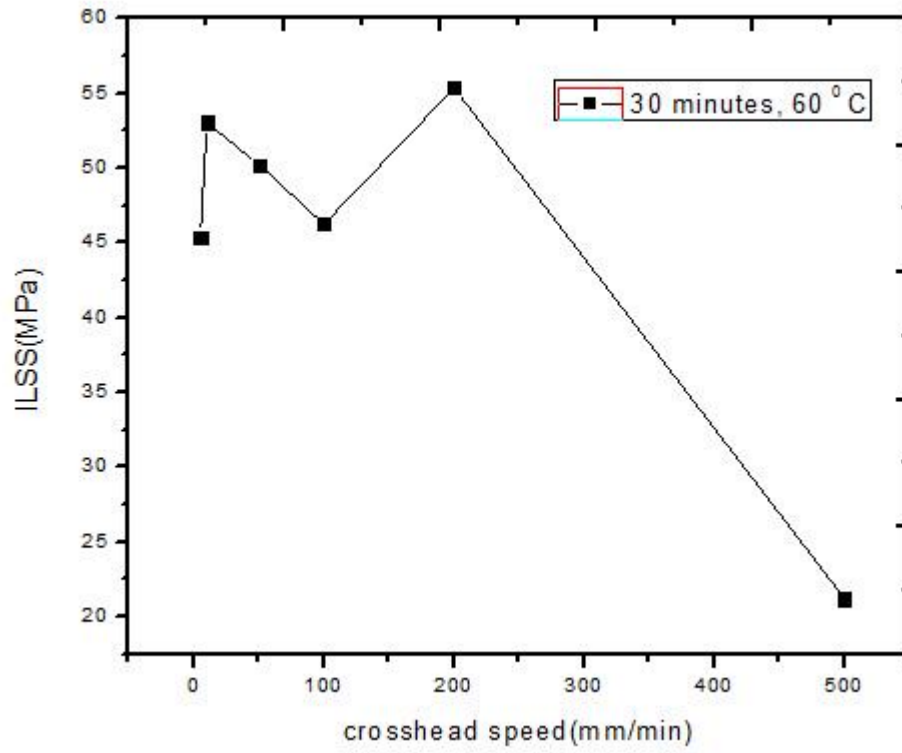


*Fig 23- ILSS Vs. Cross head speed for glass/epoxy composites at 60°C temperature conditioned for 30 minutes*

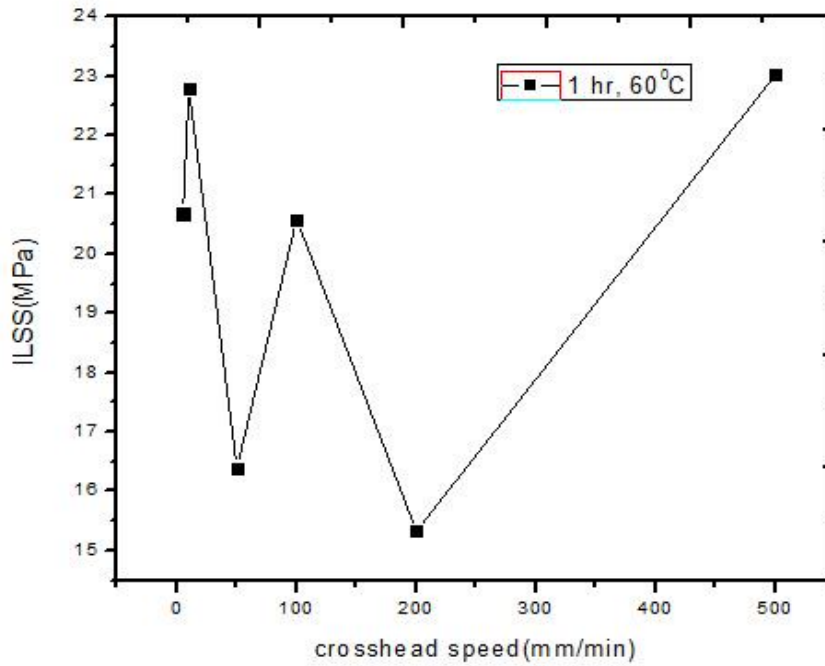


Fig 24- ILSS Vs. Cross head speed for glass/epoxy composites at 60°C temperature conditioned for 1 hour.

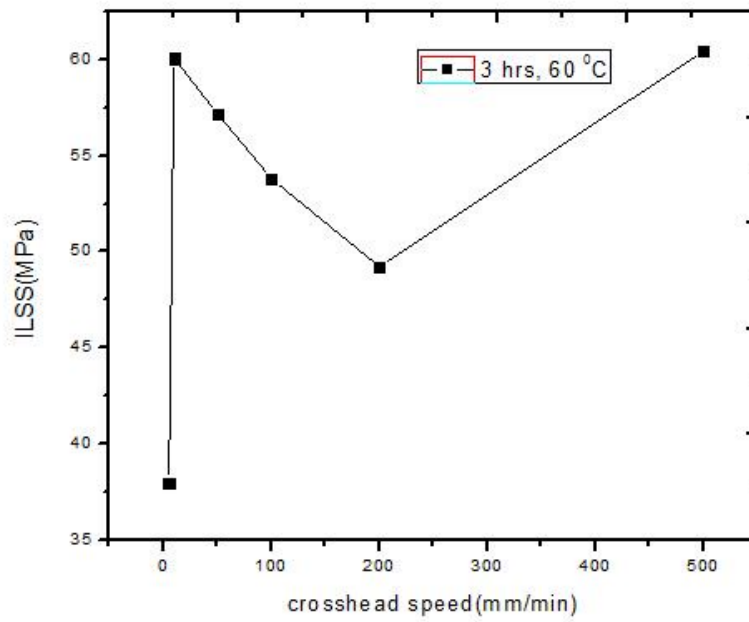


Fig 25- ILSS Vs. Cross head speed for glass/epoxy composites at 60°C temperature conditioned for 3 hour.

This implies that there is an initial increase in the ILSS or the bond strength due to increase in stiffness of the composite at lower crosshead speeds. As the crosshead speed is increased above 100mm/min, ILSS decreases due to brittle behaviour of the matrix. Relaxation time is the time required by the matrix to transfer the stress to the fiber. When crosshead speed is low, the relaxation time is long due to which efficient load transfer occurs thereby increasing the strength of the matrix. In contrast, when the crosshead speed is high, very little time is given for the transfer of the load. This is very similar to impact load. The ILSS values deteriorate due to improper transfer of load. When impact loading occurs, the gross plastic deformation is high accompanied by various modes of failure (fiber fracture, fiber pull out, matrix cracking and delamination). Now we compare the ILSS values at different temperature and conditioning time for a given cross head speed.

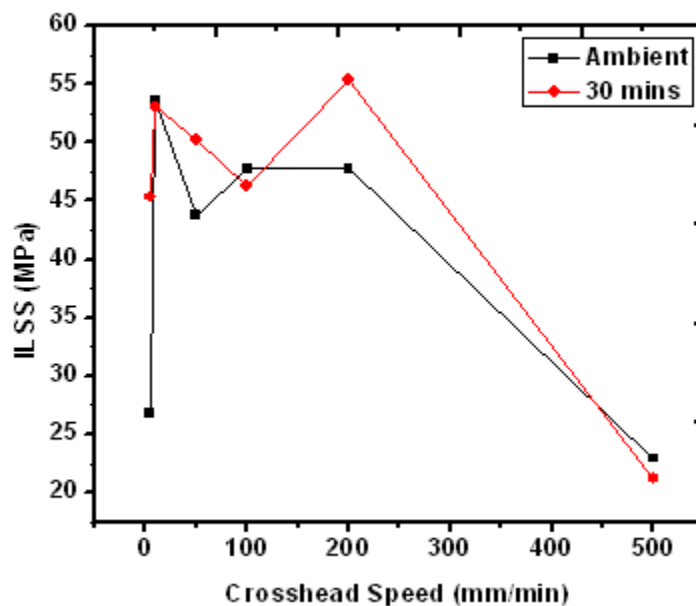
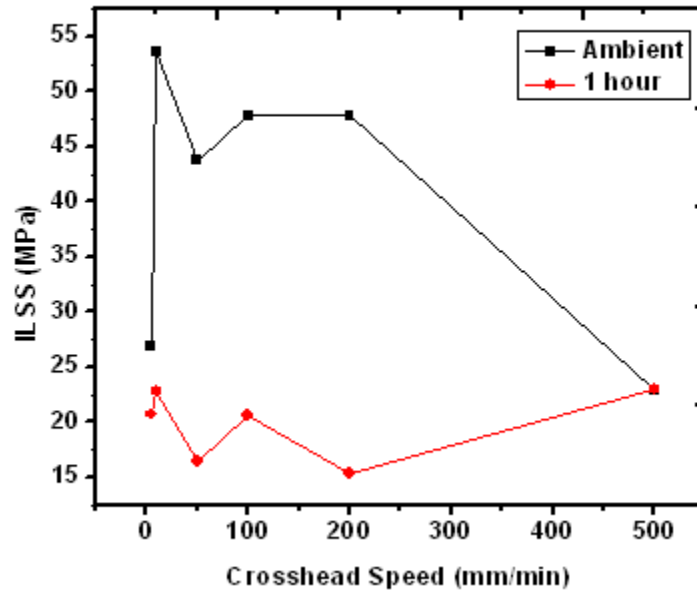


Fig 26- ILSS Vs. Cross head speed for glass/epoxy composites at ambient and at 60°C temperature conditioned for 30 minutes.

There is a relative increase in the ILSS value as thermal conditioning is done for 30 minutes which is shown in Fig 26. This is attributed to the further polymerization techniques which stiffen the matrix and enhance the curing effects. The adhesion becomes stronger.



*Fig 27- ILSS Vs. Cross head speed for glass/epoxy composites at ambient and at 60°C temperature conditioned for 1 hour*

The comparison of the specimen at ambient temperature and 60°C for 1 hour in Fig 27. There is a decrease in ILSS values. The explanation is attributed to the fact that residual stresses develop due to differential expansion of matrix and fibre. The fibre is under compression where as matrix is under tension. This weakens the interfacial bond and hence, delamination occurs.



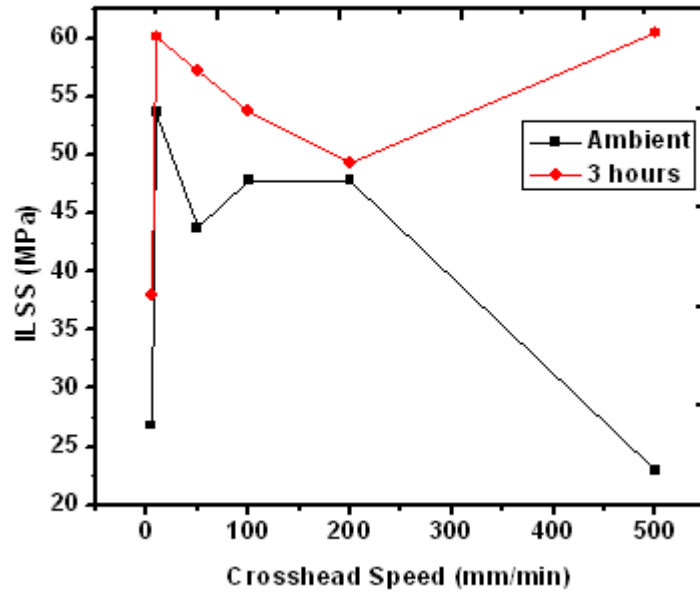


*Fig 28- ILSS Vs. Cross head speed for glass/epoxy composites at ambient and at 60°C temperature conditioned for 3 hour*

In Fig 28 the comparison of ILSS values is done for ambient temperature and 60°C for 3 hours. There is a rise in the ILSS values. When the conditioning time is 3 hours, apart from further polymerization, penetrating and semi penetrating networks are formed at the interface. It is basically permanent chain entanglement and cross linking along with fusion and coagulation of polymer lattices.

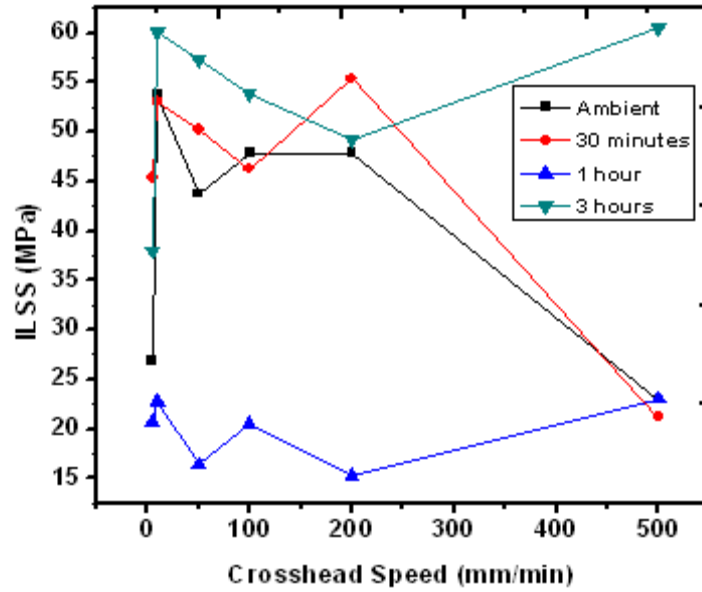


*Fig 29- ILSS Vs. Cross head speed for glass/epoxy composites at ambient and at 60°C temperature conditioned for 30minutes, 1 hour and 3hours.*

The superimposition of the ILSS vs. Crosshead speed curves for ambient and 60°C for 30 minutes, 1hour and 3 hours is done in Fig 29.

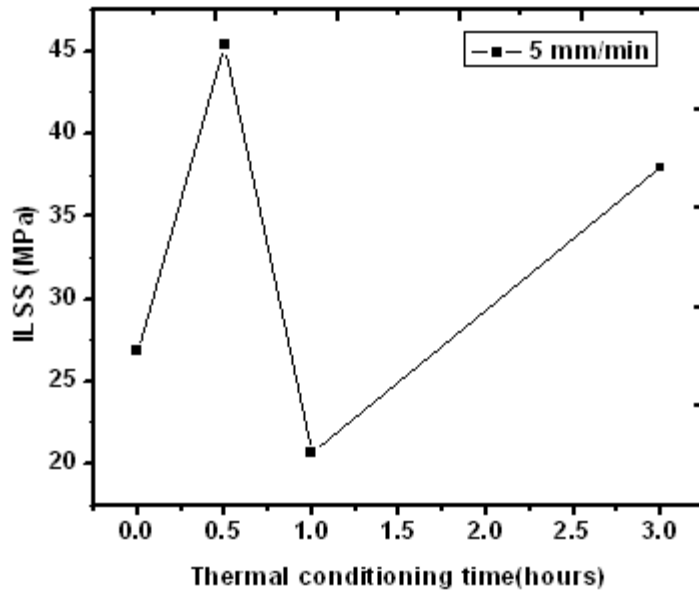


Fig 30- ILSS vs. conditioning time for glass/epoxy composites at the crosshead speed of 5mm/min

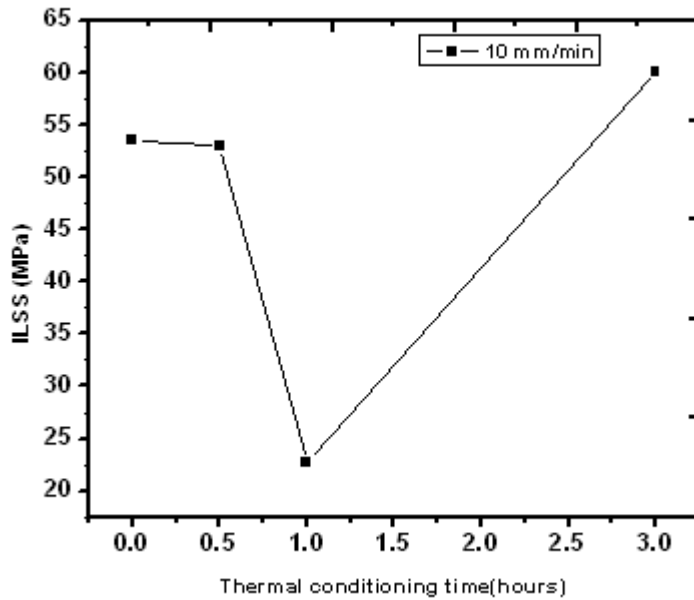


Fig 31- ILSS vs. conditioning time for glass/epoxy composites at the crosshead speed of 10mm/min

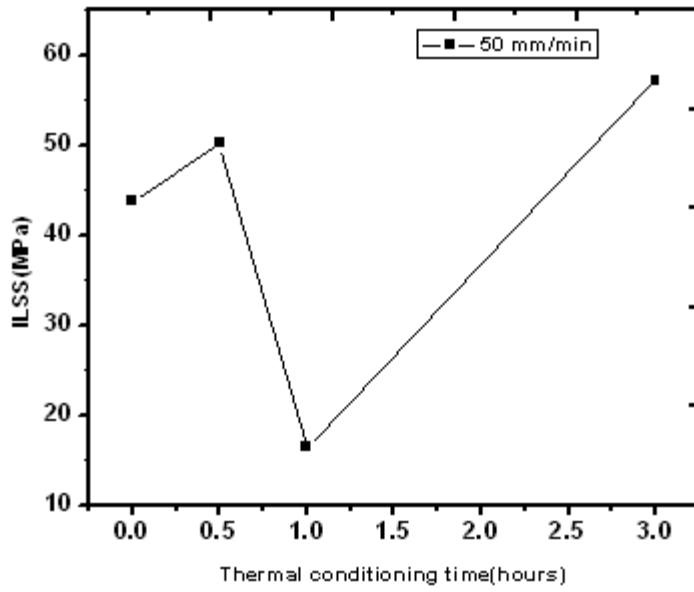


Fig 32- ILSS vs. conditioning time for glass/epoxy composites at the crosshead speed of 50mm/min

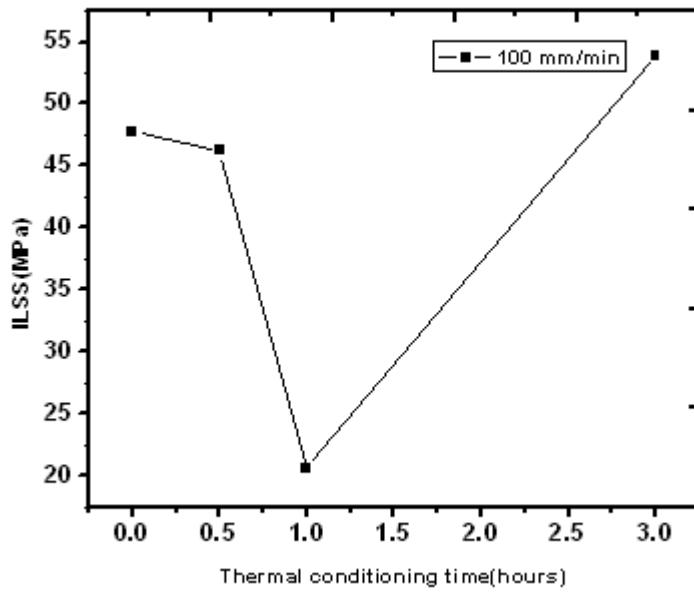


Fig 33- ILSS vs. conditioning time for glass/epoxy composites at the crosshead speed of 100mm/min

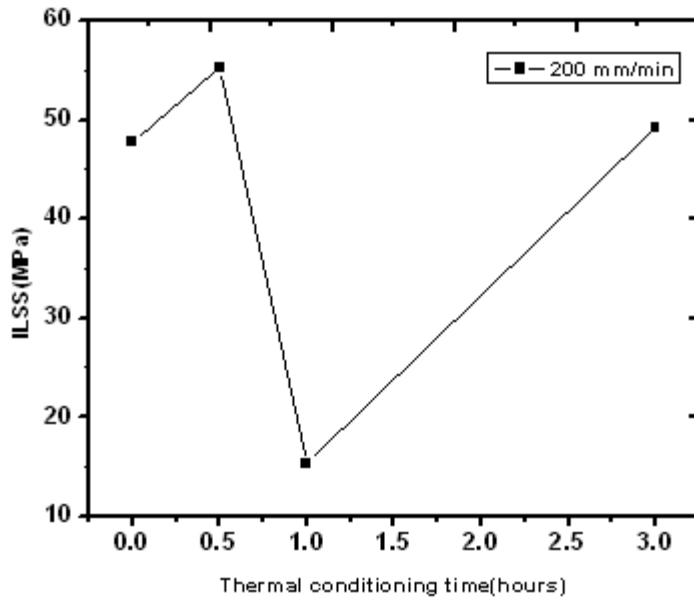


Fig 34- ILSS vs. conditioning time for glass/epoxy composites at the crosshead speed of 200mm/min

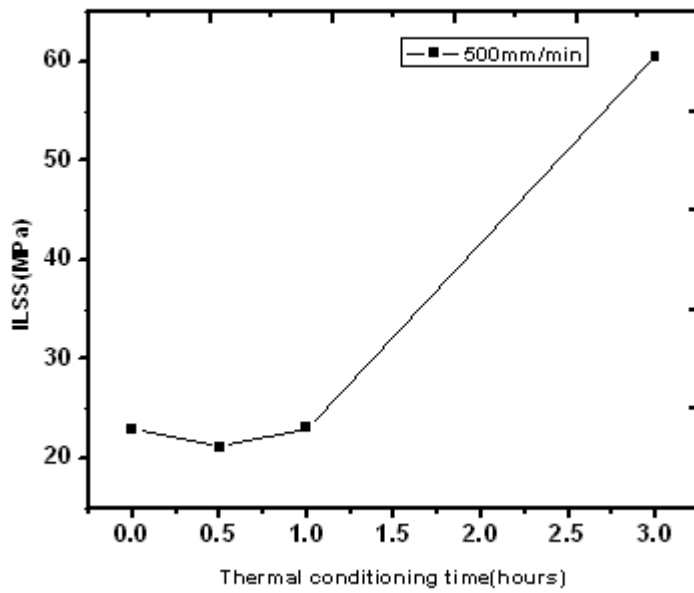


Fig 35- ILSS vs. conditioning time for glass/epoxy composites at the crosshead speed of 500mm/min

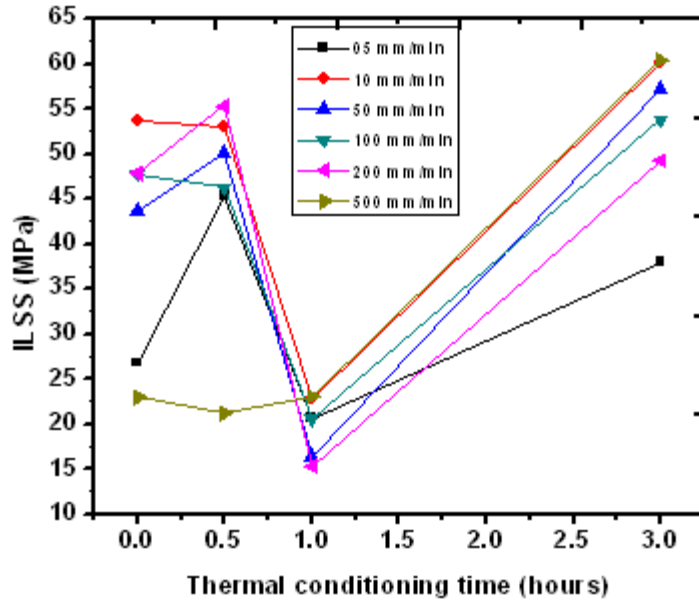


Fig 36- ILSS Vs. conditioning time for glass/epoxy composites at the crosshead speed of 5mm/min, 10mm/min, 50mm/min, 100mm/min, 200mm/min and 500mm/min

Figure 30-35 compares the ILSS values for varying conditioning times for a given crosshead speed at above ambient temperature, further polymerization occurs and the adhesion between fiber and matrix improves due to better bonding. As time increases, there is a rise in the ILSS value up to 1 hour. At 1 hour ILSS value seems to have an inflexion which can be explained by the dominance of residual stress in the composite due to differential coefficients of thermal expansion of matrix and fiber, which leads to debonding and decrease in ILSS. Further increase in conditioning time is supposed to increase ILSS value because along with polymerization, penetrating and semi penetrating layers are formed at the interface. This enhances the adhesion and bond strength between fiber and matrix. . The pattern is the same for each loading rate. Fig 36 is the superimposition of the graphs in Fig 30-35 showing ILSS vs. conditioning time at 60°C for a given crosshead speed. Their relative comparison tallies with the results of varying crosshead speed and ILSS values as explained above.

**Table 4-Strain at Yield/Peak at different crosshead speeds for thermally conditioned samples for a given conditioning time and ambient samples**

<b>Crosshead Speed</b>  <b>(mm/min)</b>	<b>Strain at Yield</b>  <b>Ambient</b>  <b>(mm/mm)</b>	<b>Strain at Yield</b>  <b>60°C,30 minutes</b>  <b>(mm/mm)</b>	<b>Strain at Yield</b>  <b>60°C, 1 hour</b>  <b>(mm/mm)</b>	<b>Strain at Yield</b>  <b>60°C, 3 hours</b>  <b>(mm/mm)</b>
<b>5</b>	0.0230	0.0163	0.0320	0.0205
<b>10</b>	0.0190	0.0022	0.0281	0.0150
<b>50</b>	0.0020	0.0021	0.0075	0.0039
<b>100</b>	0.0039	0.0045	0.0074	0.0066
<b>200</b>	0.0092	0.0096	0.0137	0.0085
<b>500</b>	0.0391	0.0331	0.0413	0.0196

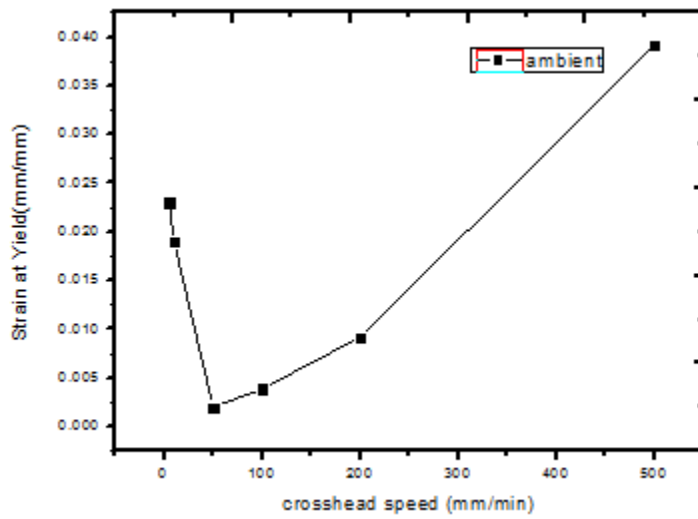


Fig 37 – Strain at Yield Vs. Crosshead Speed for samples at ambient temperature

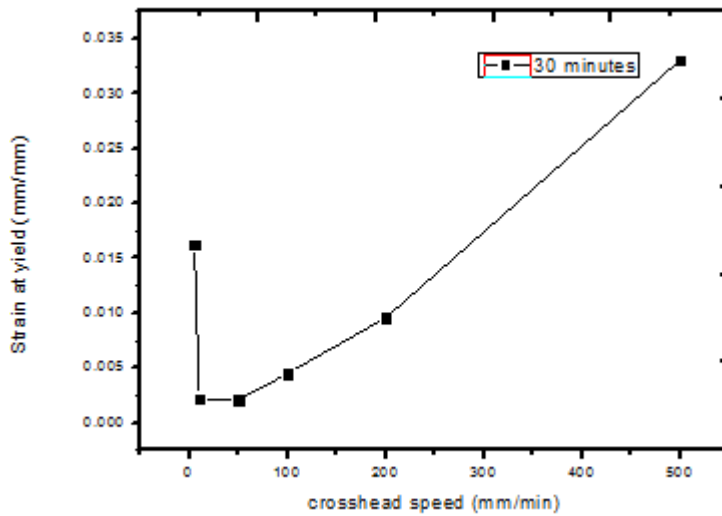


Fig 38- Strain at Yield Vs. Crosshead Speed for samples thermally conditioned at 60°C for 30 minutes



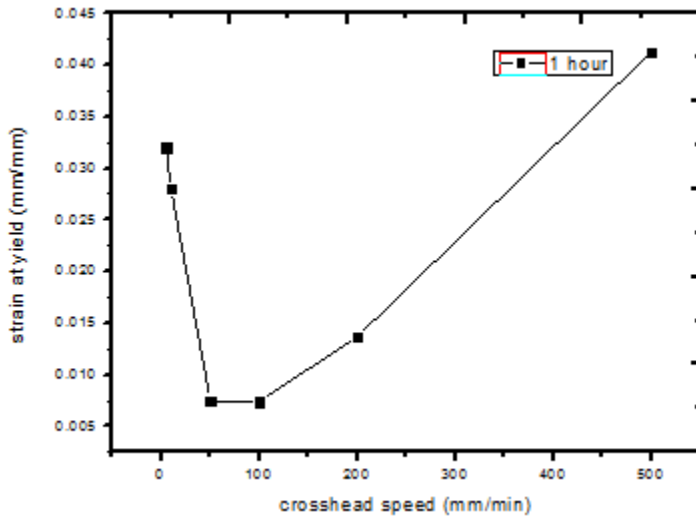


Fig 39 - Strain at Yield Vs. Crosshead Speed for samples thermally conditioned at 60°C for 1 hour

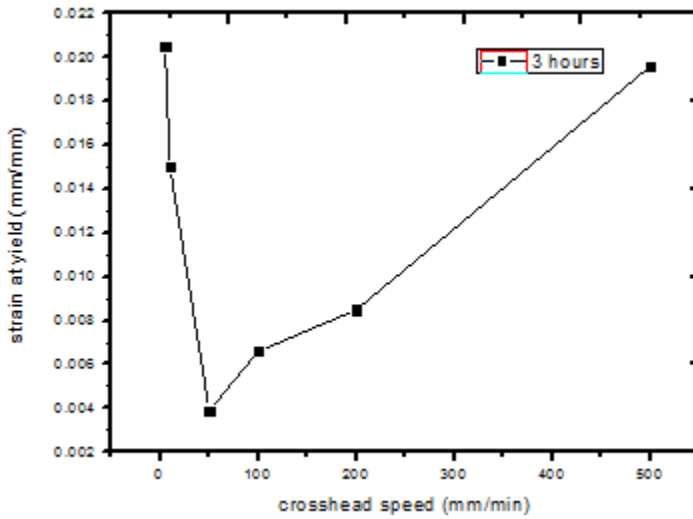


Fig 40 - Strain at Yield Vs. Crosshead Speed for samples thermally conditioned at 60°C for 3 hours

With thermal conditioning is done, the matrix becomes brittle and harder due to further polymerization and crosslinking. The ductility reduces which is reflected by reduction in strain at yield or peak .

## 4.2 SEM Analysis

There are four major failure modes in the fibre reinforced composites, namely, fibre cracking, matrix cracking, delamination and fiber pullout.

1. Fibre cracking: Due to the presence of surface flaws in the fiber, cracks might be generated in the fiber. This will lead to fiber failure.
2. Matrix cracking: When stress is not transferred to the fibre due to lack of relaxation time or insufficient adhesion between the fibre and the matrix, the matrix yields under load.
3. Delamination: The fibre and matrix layers separate due to weak interfacial bonding. Shear stresses act on the interface and the debonding occurs.
4. Fibre pullout: The embedded fibre in the matrix is pulled out when tensile force is applied.

**SEM images showing modes of failure in GFRP composites**

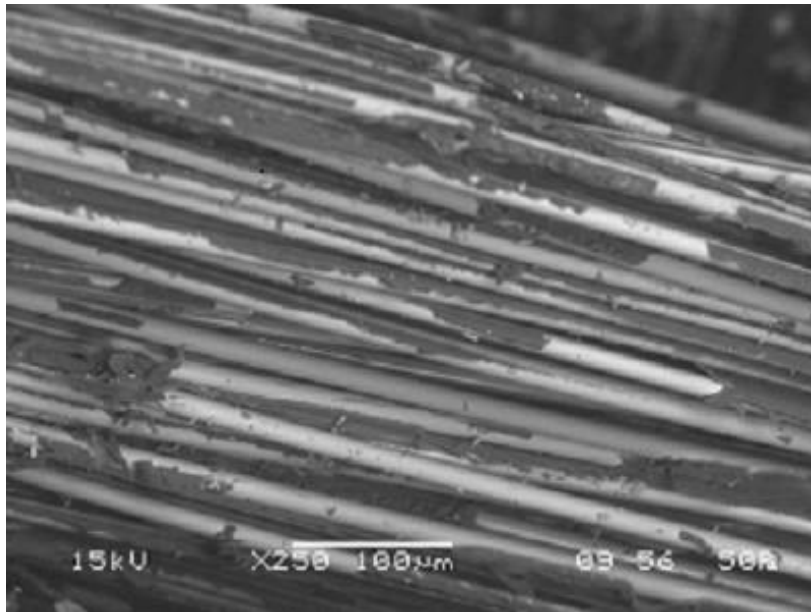


*Fig 41- SEM Micrograph showing strong fiber matrix interface*

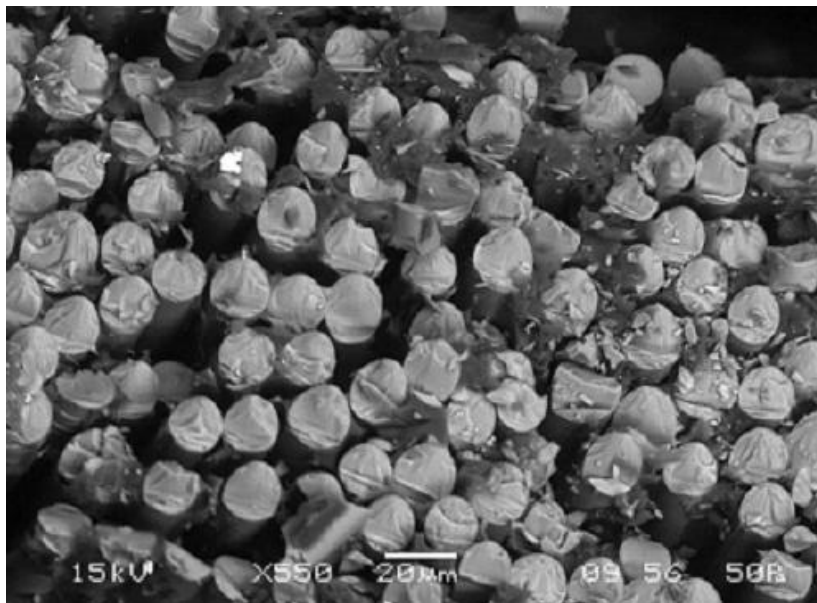


*Fig 42- SEM Micrograph showing a weak interface which leads to failure mechanism of fiber pullout*

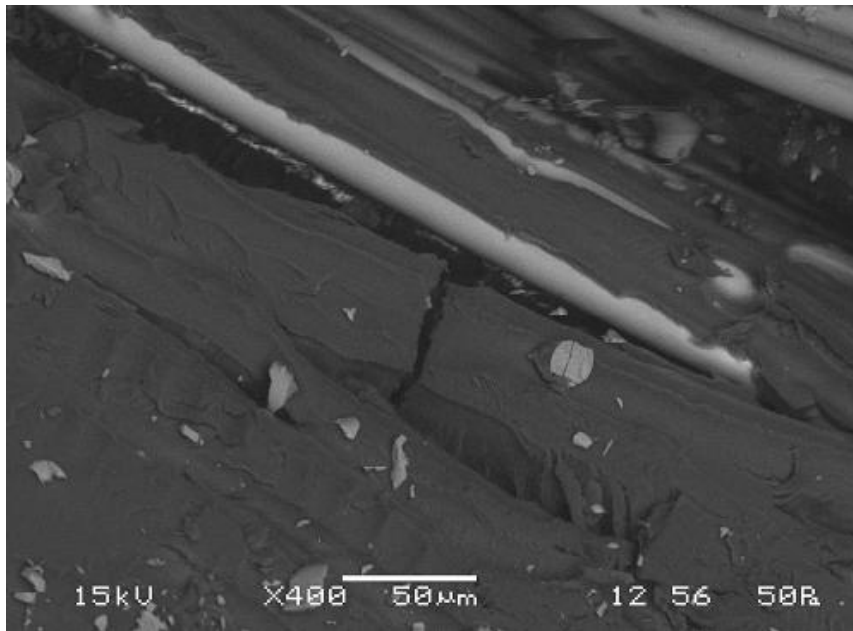


*Fig 43- SEM micrograph showing strong interface which leads to matrix cracking*

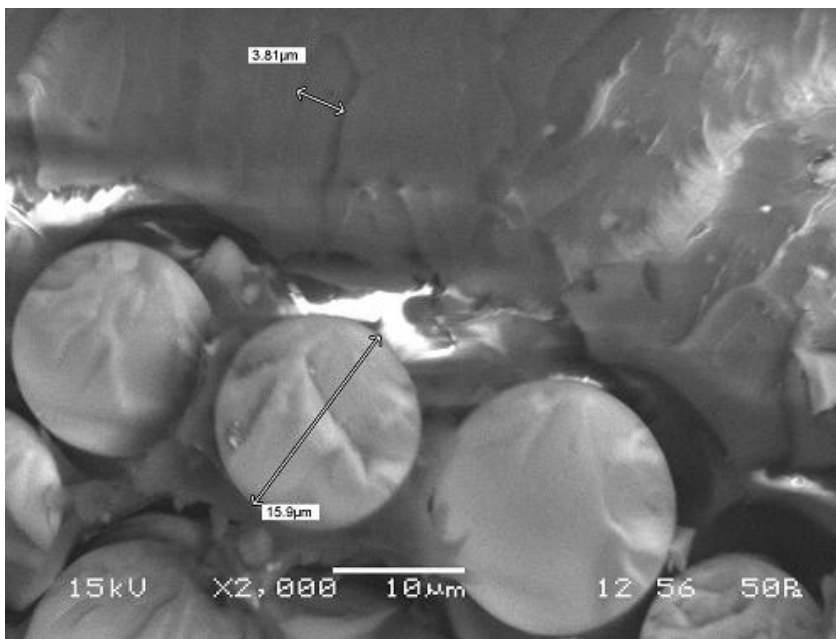


*Fig 44- SEM micrograph showing weak interface and the mechanism of debonding*

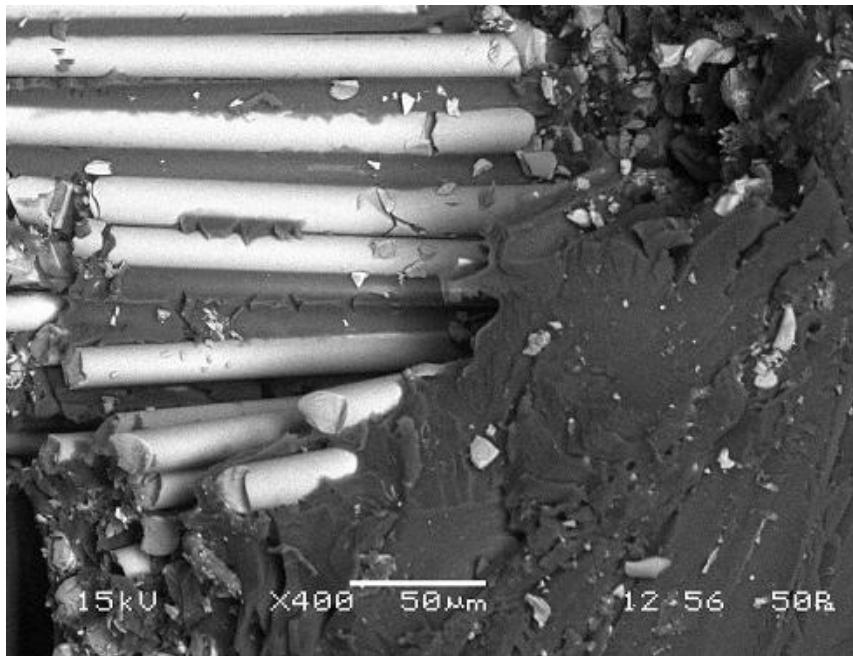


*Fig 45- SEM micrograph showing fiber pullout and extensive matrix damage*

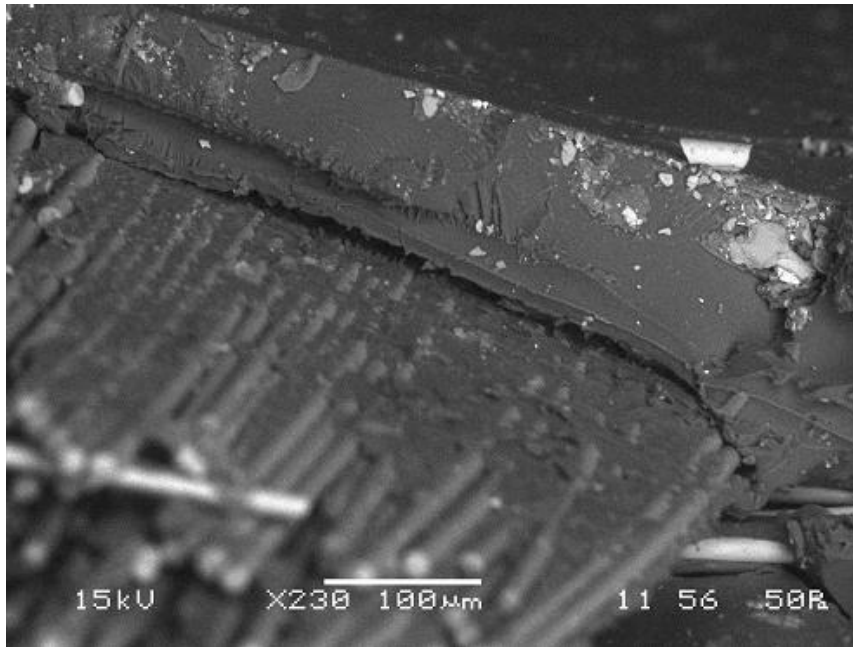


*Fig 46- SEM micrograph shows a strong interface giving rise to failure mechanisms like matrix cracking at 60°C for 30 minutes*

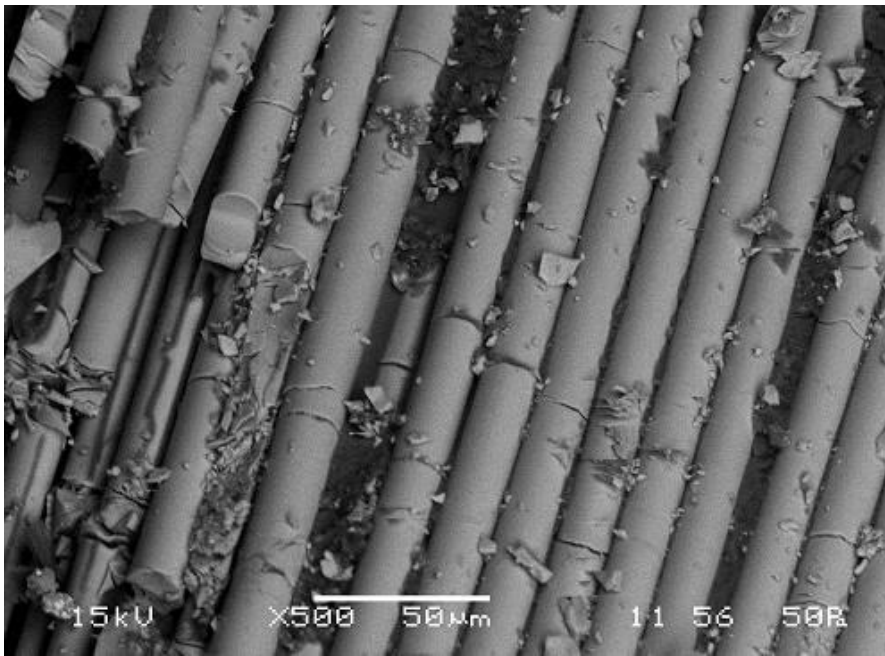


*Fig 47- SEM micrograph showing fiber cracking*

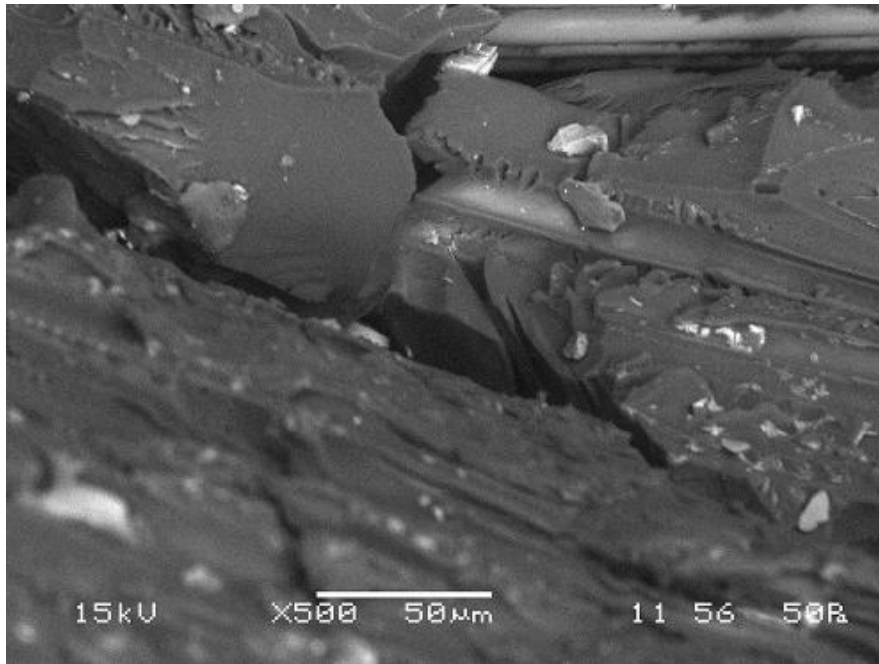


*Fig 48 - SEM micrograph showing fractured surface with cusps*

As temperature increases, further polymerization occurs which renders the matrix brittle in nature. Due to this there is micro and macrocracking of matrix. There is also an improvement in the interfacial

bonding. As we increase the conditioning time to around 1 hour, residual stresses of higher order are generated. This causes delamination of composite and fiber pullout. Further increase in conditioning time strengthens the interface by formation of penetrating and semi-penetrating networks at the interface. So failure mechanisms chiefly involves fiber fracture and matrix cracking. The matrix failure is brittle in nature as striations, cusps and rivet markings are observed in the matrix as shown in Fig 48.

### **4.3 FTIR measurement**

The micro-voids may be formed during curing or stresses generated due to difference in thermal expansion coefficient between the glass fiber and the epoxy matrix at the interface enhances the moisture absorption. In FTIR, the shift of spectra may reveal information on micro changes or micro degradation of fibre/polymer interphase of composites. The interfacial region where stress concentration develop because of difference in the thermal expansion coefficient between the reinforcement and the matrix phase due to loads applied to the structure and the time of curing shrinkage. Thus a concise and critical assessment of the interphase is an utmost necessary to decisively and precisely evaluate and predict the structural durability and integrity of a composite structure.

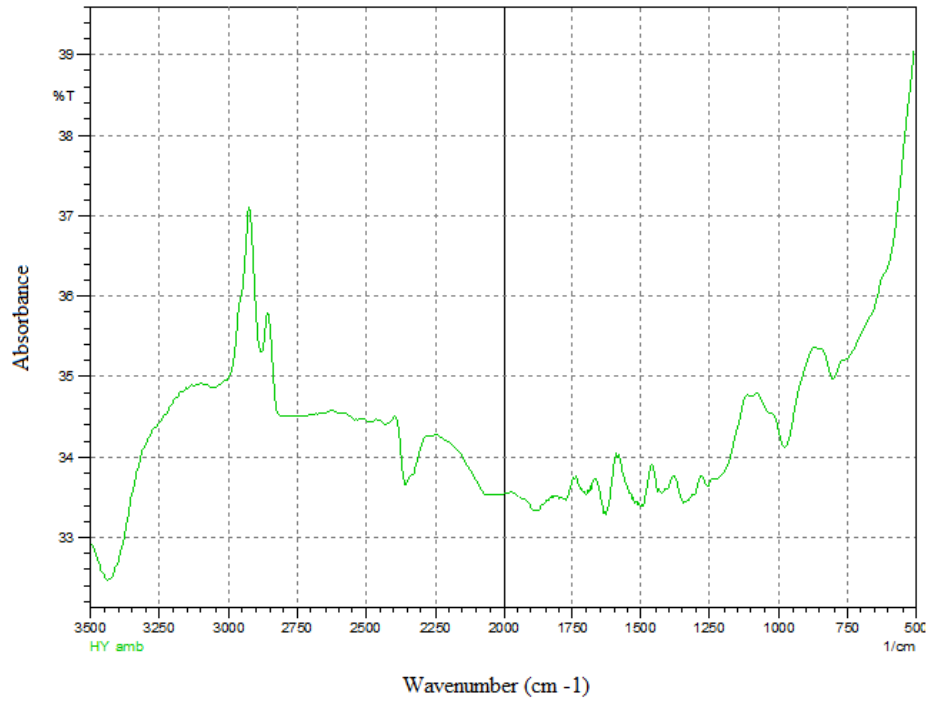


Fig 49 - 2D micrographs taken by FTIR spectrophotometer of untreated glass/epoxy composites

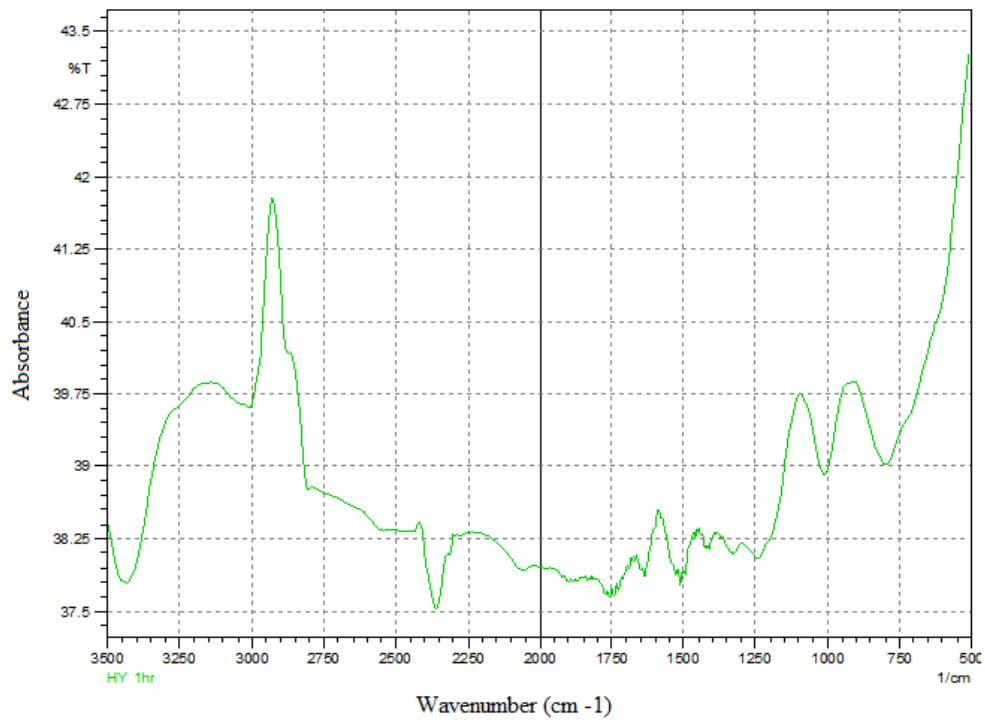




Fig 50 - 2D micrographs taken by FTIR spectrophotometer of hygroscopically treated glass/epoxy composites at 1 Hr

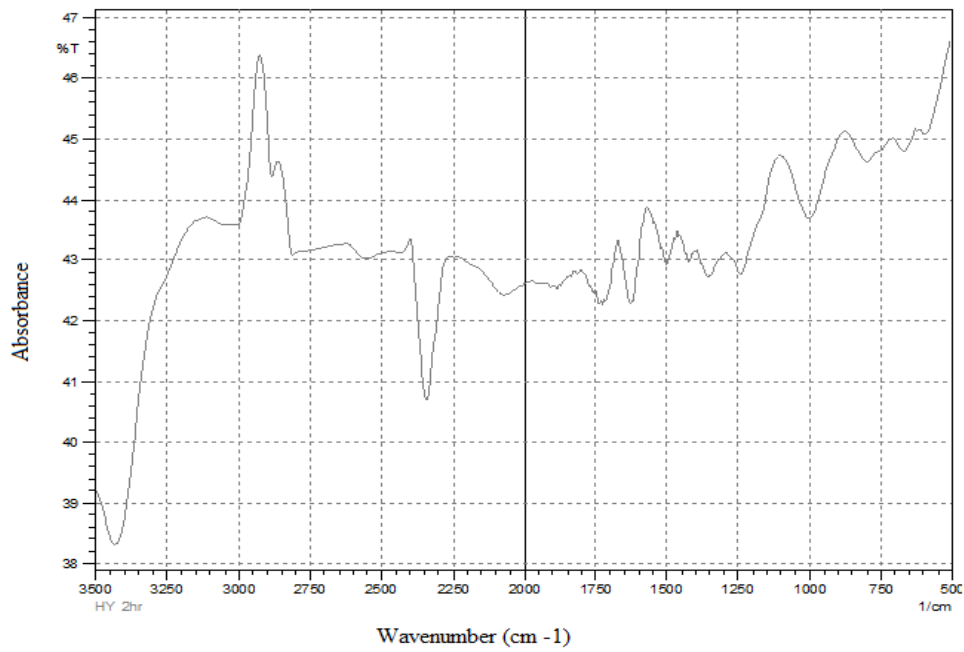
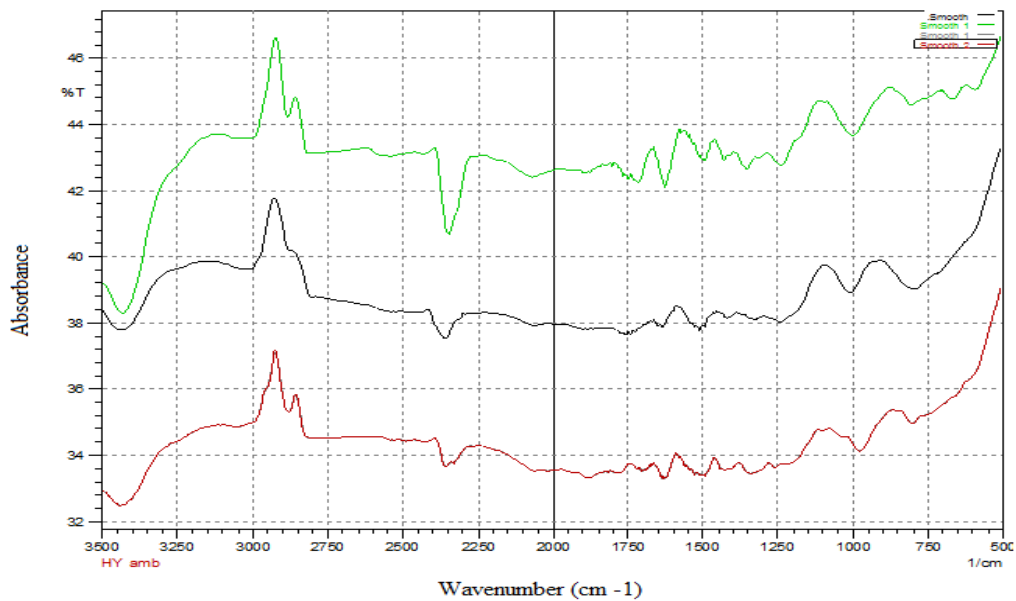


Fig 51-2D micrographs taken by FTIR spectrophotometer of hygroscopically treated glass/epoxy composites at 2 Hr



*Fig 52 - 2D micrographs taken by FTIR spectrophotometer of untreated(red), hygroscopically treated glass/epoxy composites at 1 Hr(black) and , hygroscopically treated glass/epoxy composites at 2 Hr(green)*

The duration of water penetration during hygrothermal treatment increases, the absorbance in the 2D micrograph increases which is well depicted in Fig 52.

#### **4.4 DSC measurements**

Polymer composites are used at a temperature below their glass transition temperature as above the glass transition temperature, the matrix gets softened and exhibit visco-elastic behavior. DSC analysis shows an increase in glass transition temperature ( $T_g$ ) with thermal conditioning for glass/epoxy composites. But with increase in thermal conditioning time the  $T_g$  increases. During thermal conditioning higher polymerization occur which results in formation of interpenetrating and/or semi-penetrating networks. This delays the transition from glassy to rubbery and hence, the glass transition temperature increases.

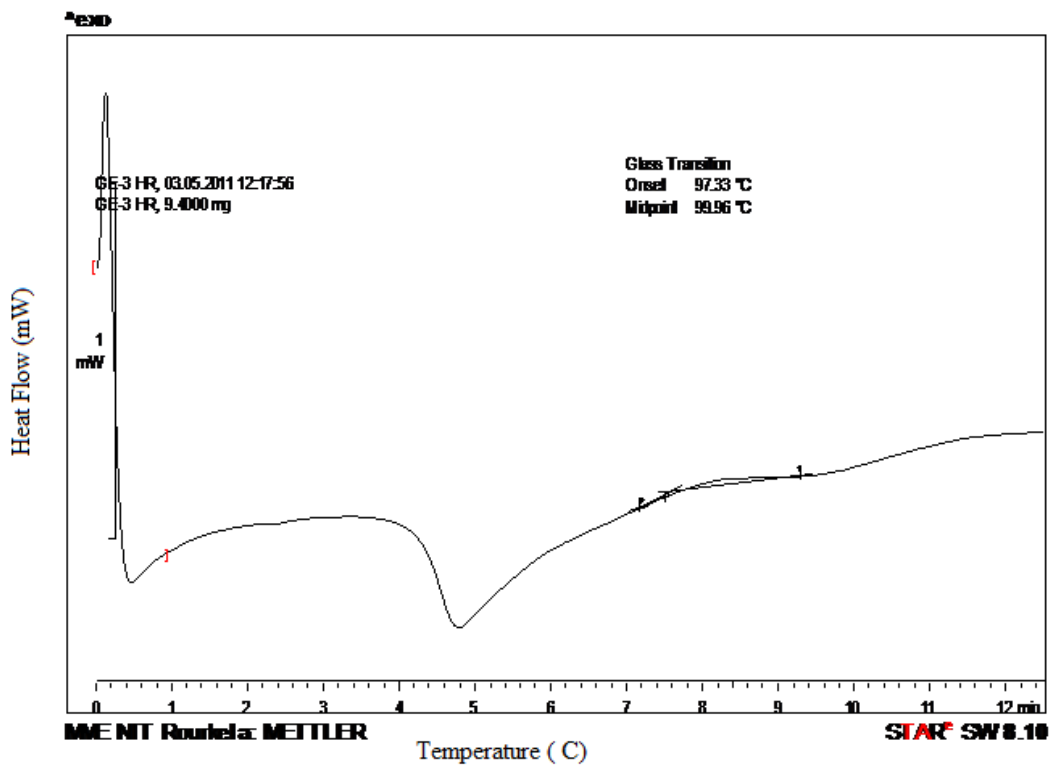


Fig 53- DSC plot:  $T_g$  vs. Temperature for GFRP sample at ambient temperature

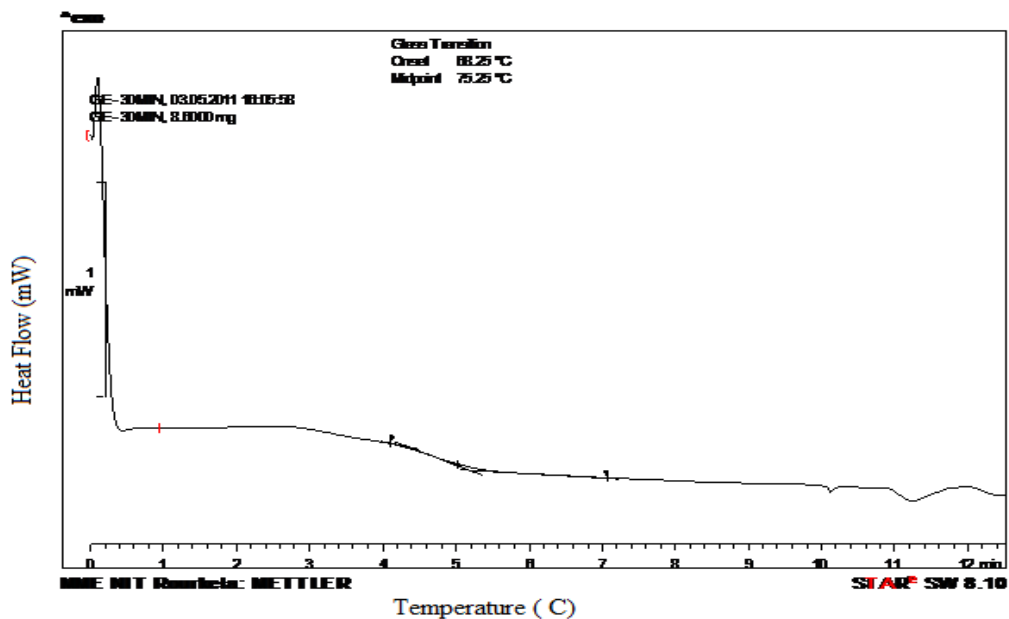


Fig 54- DSC plot:  $T_g$  vs. Temperature for GFRP sample thermally conditioned at 60°C for 30 mins

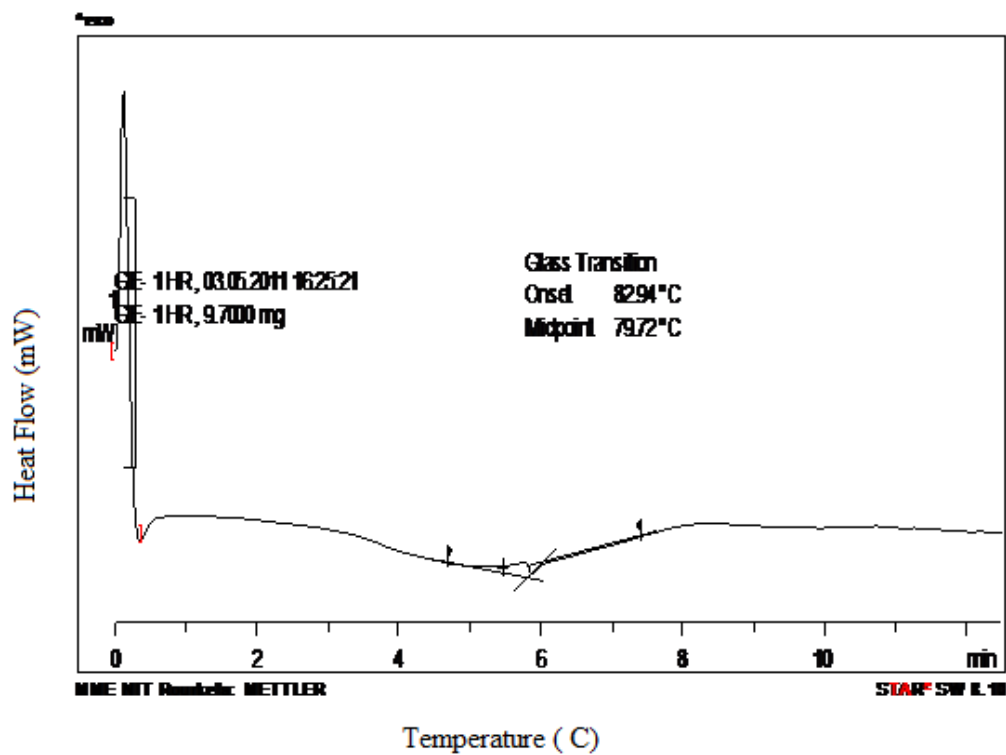


Fig 55- DSC plot: Tg vs. Temperature for GFRP sample thermally conditioned at 60°C for 1 hour

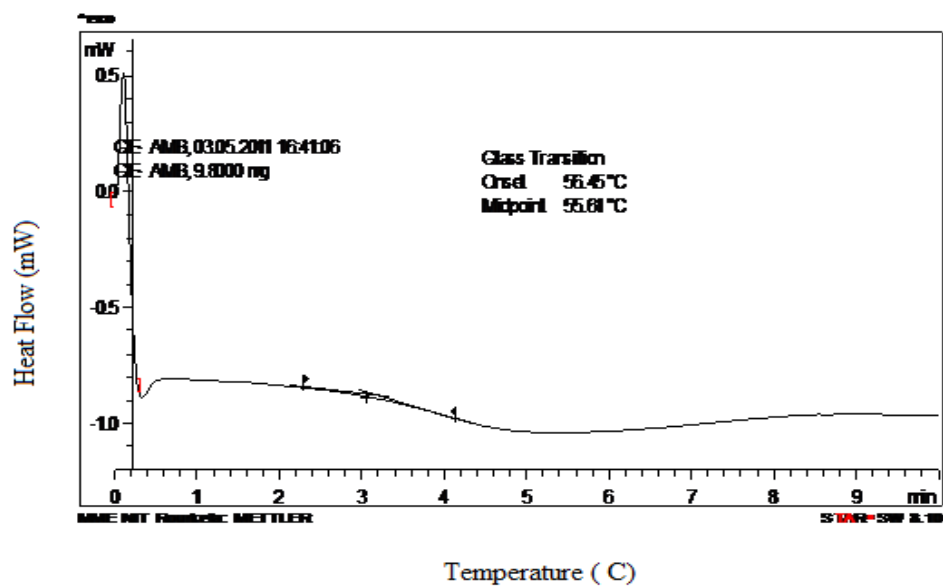
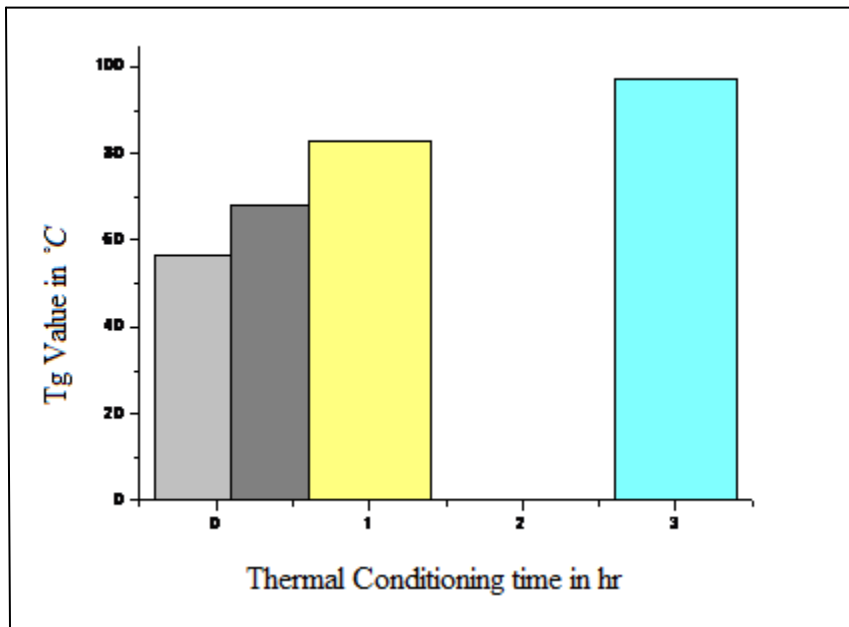


Fig 56- DSC Plot: Tg vs. Temperature for GFRP sample thermally conditioned at 60°C for 3 hours

**Table 5- Tg Vs thermal conditioning time for glass/epoxy composite**

<b>Thermal conditioning time (Hrs)</b>	<b>Tg (°C) for glass/epoxy</b>
<b>0</b>	<b>56.45</b>
<b>0.5</b>	<b>68.25</b>
<b>1</b>	<b>82.94</b>
<b>3</b>	<b>97.33</b>



*Fig 57- Bar Chart showing Tg Vs Thermal conditioning time for glass/epoxy composites at 60°C*

It is shown in Fig 57 that the Tg value increases with increase in conditioning time. With increasing Tg the ILSS may increase initially. Hence we are tempted to assume that there is enhancement of mechanical properties.

# CHAPTER-5

# CONCLUSION

1. The three major parameters may affect the mechanical properties of composite, namely, crosshead speed, temperature and conditioning time.
2. The effect of crosshead speed is varied. Initial rise in the crosshead speed increases the ILSS value as the relaxation time is high, which causes proper transfer of load from matrix to fibre. At higher crosshead speed, ILSS decreases due to low relaxation time.
3. As temperature increases, there is improvement in the interfacial bonding and ILSS increases. However, with an increase in the conditioning time, there is a fluctuation in ILSS values. There is a decrease followed by an increase in ILSS. The decrease in ILSS is attributed to differential thermal expansion of matrix and fibre leading to induction of residual stress in the interface. This leads to weakening of bond strength. After this decrease there is another inflection in ILSS due to stronger interface as semi penetrating and penetrating networks form at the interface.
4. The interface is the key to understand the mode of failure of composite. When the interface is strong, the failure occurs by fibre fracture and matrix cracking. When the interface is weak, debonding and delamination occurs.
5. When temperature increase, further polymerization embrittles the matrix. This is why the matrix failure is brittle in nature.
6. FTIR spectroscopy analysis shows that the absorption spectra is affected by the presence on water molecules.
7. DSC result depicts that the glass transition increases with increase in thermal conditioning time.



## References

1. ASM Handbook, J.Composites (ASM International),21(2001)
2. Callister, W D., Materials Science and Engineering: An Introduction. Asia, John Wiley and Sons,7 (2007)
3. Dalai, Renu Prava , An Assessment of Mechanical Behavior of Fibrous Polymeric Composites Under Different Loading Speeds at Above- And Sub-Ambient Temperatures. Ray, B.C, NIT Rourkela, M.Tech thesis(2010).
4. Kim, K.J., Mai Y W., Engineered Interfaces in Fiber Reinforced Composites. Kidlington, Oxford, Elsevier Publication,1(1998)
5. Jang, B Z., Advanced Polymer Composites: Principle and Applications, ASM International, Materials Park,2 (1994)
6. Lee, S M., Handbook of Composite Materials. New York: VCH Publishers,2(1993)
7. Chawla, K.K., Composite Materials: Science and Engineering, USA, Springer Science + Business Media Inc.,2(1998)
8. Ray, B.C., Adhesion of Glass/Epoxy Composites Influenced by Thermal and Cryogenic Environments,J. of Applied Polymer Science,102(2006),pp.1943-1949
9. Hodzic, A.; Kim, J.K.; Lowe, A.E.; Stachurski, Z.H.,J. Composite Science and Technology, 64(2004), pp. 2185
10. Zulkifli, R., Surface fracture Analysis of Glass Fiber reinforced epoxy Composites Treated with different Type of Coupling Agent, J. Scientific Research,29(2009),pp.55-65
11. Ray, B.C., Temperature effect during humid ageing on interfaces of glass and carbon fibers reinforced epoxy composites, J. Colloid and Interface Science 298,(2006),pp.111-117.

12. Kanchanomai C, Rattananon S, Soni M. Effects of loading rate on fracture behavior and mechanism of thermoset epoxy resin, *J. Polymer Testing*, 24( 2005) :pp.886- 892
13. Hamouda, A M S, Hashmi, M S J. Testing of composite materials at high rates of strain: advances and challenges,*J. Materials Processing Technology*, 77(1998):pp. 327-336
14. Tanoglu, M, McKnight, S H, Palmese, G R and Gillespie, J W. A new technique to characterize the fiber/matrix interphase properties under high strain rates, *J. Composites Part A*, 31 (2000):pp.1127-1138.
15. Okoli, O I. The effects of strain rate and failure modes on the failure energy of fibre reinforced composites, *J. Composite Structure*, 54(2001):pp.299-303
16. Ray,B.C., Effect of Crosshead Velocity and Sub-Zero temperature on Mechanical behaviour of Hygrothemally Conditioned Glass fiber reinforced Epoxy Composite,*J. Materials Science and Engineering A*, 379(2004),pp.39-44
17. Kim, J.K. ,Mackey, , D.B. , Mai, Y.W. ,*J. Composites* 24 (1993)
18. Abdel-Magid, B, Ziaee, S, Gass, K, Schneide,r M. The combined effects of load, moisture and temperature on the properties of E-glass/epoxy composites,*J. Composite Structures*,71(2005): pp 320-326
19. Kellogg, K G, Patil, R, Kallmeyer, A R, Dutta, P K. Effect of Load Rate on Notch Toughness of Glass FRP Subjected to Moisture and Low Temperature , *J. Offshore and Polar Engineering*, 15(1), (2005):pp.54–61
20. Naruse, T, Hattori, T, Miura, H, Takahashi, K. Evaluation of thermal degradation of unidirectional CFRP rings,*J. Composite Structures* 52(2001), pp.533-538
21. Colin, X, Verdu, J. Strategy for studying thermal oxidation of organic matrix composites,*J.*

- Composite Science and Technology, 65(3-4) (2005):pp.411-419
22. Hartwig, G., Polymer properties at room and cryogenic temperatures. New York, Plenum Press,3(1994)
  23. Livshin,S., Silverstein,M.S., Crystallinity and Cross-Linking in Porous Polymers Synthesized from Long Side Chain Monomers through Emulsion Templating, J. Macromolecules 2008, 41, pp.3930-3938.
  24. Barjasteh, E, Bosze, E J, Tsai, YI, Nutt, S R. Thermal aging of fiberglass/carbon-fiber hybrid composites, Composites Part A, 40 (2009):pp.2038- 2045
  25. Borje, A, Aders, S and Lars, B. Micro- and meso- level residual stresses in glass/vinyl-ester composite, Composite Science and Technology, 60(2000):pp.2011-2028
  26. Baschek, G., Hartwig, G., Zahradnik, F., J.Polymer,40 (1999), pp.3433-344
  27. [http://www.zeusinc.com/UserFiles/zeusinc/.../Zeus\\_Low\\_Temp.pdf](http://www.zeusinc.com/UserFiles/zeusinc/.../Zeus_Low_Temp.pdf) ,Accessed[08/05/2011]
  28. [http://\\_en.wikipedia.org/wiki/Boeing\\_787\\_Dreamliner](http://_en.wikipedia.org/wiki/Boeing_787_Dreamliner) ,Accessed[08/05/2011]
  29. Ray, B.C., Sethi,S.,Interface Assessment in Composite Materials, RETMAC(2010)
  30. Lee,M.C, N.A. Peppas, J. Compos. Mater. 27(1993) ,pp.1146.
  31. Brown,E.N.,Davis, A.K., Jonnalagadda,K.D., Sottos,N.R., Compos. Sci. Technol. 65(2005) ,pp.129.
  32. Schutte, C.L., Mater. Sci. Eng. Reports: J.A Review Journal, 13(1994) ,pp.265
  33. Li,L.,Zhang,S.Y.,Liu,M.,Ding.Y.,Luo,X.W.,Pu,Z.,Zhou,W., Li,S., “Water transportation in Epoxy Resin”. J. Chemistry of Material,17(2005)pp.839.
  34. <http://onlinelibrary.wiley.com/doi/10.1002/app.24488/full>, Accessed[06/05/2011]

## APPENDIX

### SHORT BEAM SHEAR TEST RESULTS

GFRP Composite specimens at ambient temperature( untreated)

<b>Specimen No.</b>	<b>Width (mm)</b>	<b>Thickness(mm)</b>	<b>Crosshead Speed (mm/min)</b>	<b>Load at yield (KN)</b>	<b>Strain at Yield (mm/mm)</b>
1	6.000	4.000	5	0.6325	0.0260
2	6.000	4.000	5	0.7731	0.0238
3	5.000	3.000	5	0.8233	0.0192
4	4.500	2.500	10	0.7838	0.0162
5	5.000	2.500	10	0.9047	0.0127
6	4.500	2.500	10	0.6477	0.281
7	6.500	3.000	50	0.9687	0.0021
8	4.000	2.500	50	0.6357	0.0020
9	5.500	2.500	50	0.8829	0.0019
10	6.000	2.500	100	0.9138	0.0042
11	4.500	2.500	100	0.7576	0.0039
12	5.000	2.500	100	0.7979	0.0036
13	5.000	3.000	200	0.9778	0.0090
14	5.000	3.000	200	0.8765	0.0110
15	4.500	3.000	200	0.8261	0.0083
16	4.500	2.500	200	0.8009	0.0084
17	8.290	4.830	500	1.252	0.0359
18	7.540	4.590	500	1.092	0.0394
19	7.780	4.660	500	1.047	0.0420

GFRP Composite specimens conditioned at 60°C for 30 minutes

<b>Specimen No.</b>	<b>Width (mm)</b>	<b>Thickness(mm)</b>	<b>Crosshead Speed (mm/min)</b>	<b>Load at yield (KN)</b>	<b>Strain at Yield (mm/mm)</b>
<b>1</b>	6.000	3.000	5	1.0110	0.0201
<b>2</b>	6.000	2.500	5	.8632	0.0138
<b>3</b>	4.000	2.500	5	0.7051	0.0150
<b>4</b>	5.000	2.500	10	0.7891	0.0013
<b>5</b>	4.000	2.500	10	0.8871	0.0012
<b>6</b>	4.000	2.500	10	0.8092	0.0040
<b>7</b>	5.000	2.500	50	0.1975	0.0019
<b>8</b>	4.000	2.000	50	0.3567	0.0027
<b>9</b>	4.000	3.000	50	0.1648	0.0019
<b>10</b>	6.000	3.000	100	0.9727	0.0045
<b>11</b>	4.000	2.500	100	0.6570	0.0043
<b>12</b>	4.000	2.500	100	0.6549	0.0046
<b>13</b>	5.000	2.000	200	0.8566	0.0069
<b>14</b>	4.000	2.500	200	0.6550	0.0096
<b>15</b>	3.000	2.500	200	0.5542	0.0123
<b>16</b>	7.960	4.870	500	1.067	0.0315
<b>17</b>	7.880	4.690	500	1.037	0.0319
<b>18</b>	8.790	4.650	500	1.192	0.0358

GFRP Composite specimens conditioned at 60°C for 1 hour

<b>Specimen No.</b>	<b>Width (mm)</b>	<b>Thickness(mm)</b>	<b>Crosshead Speed (mm/min)</b>	<b>Load at yield (KN)</b>	<b>Strain at Yield (mm/mm)</b>
1	7.140	4.860	5	0.9524	0.0284
2	8.380	5.190	5	1.2350	0.0382
3	7.370	4.820	5	0.9423	0.0294
4	7.560	5.440	10	1.145	0.0254
5	8.560	4.810	10	1.251	0.0255
6	7.030	4.710	10	1.115	0.0333
7	7.650	4.760	50	0.8181	0.0071
8	7.580	4.720	50	0.7780	0.0124
9	7.640	4.500	50	0.7330	0.0030
10	6.930	4.560	100	0.9075	0.0070
11	7.690	4.580	100	0.8925	0.0072
12	7.390	4.730	100	0.9928	0.0078
13	8.400	4.590	200	0.8832	0.0140
14	8.000	4.590	200	0.4467	0.0053
15	7.720	4.810	200	0.9685	0.0219
16	8.700	4.620	500	1.194	0.0357
17	8.620	4.530	500	1.179	0.0315
18	7.920	4.460	500	1.144	0.0566

GFRP Composite specimens conditioned at 60°C for 3 hours

<b>Specimen No.</b>	<b>Width (mm)</b>	<b>Thickness(mm)</b>	<b>Crosshead Speed (mm/min)</b>	<b>Load at yield (KN)</b>	<b>Strain at Yield (mm/mm)</b>
1	5.000	3.000	5	0.9639	0.0241
2	6.000	3.000	5	0.9337	0.0197
3	6.000	3.000	5	0.9689	0.0176
4	5.000	2.500	10	0.9239	0.0183
5	5.000	2.000	10	0.8888	0.0112
6	5.500	2.500	10	1.0850	0.0153
7	7.350	4.800	50	0.9505	0.0039
8	6.000	4.000	100	1.277	0.0090
9	5.000	3.000	100	1.167	0.0067
10	5.000	2.500	100	1.192	0.0042
11	6.000	3.000	200	1.0590	0.0080
12	5.000	3.000	200	0.9484	0.0107
13	5.000	2.500	200	0.9685	0.0069
14	5.000	2.000	500	0.9053	0.0194
15	6.000	2.500	500	1.1560	0.0201
16	6.000	2.500	500	1.1360	0.0192